

See discussions, stats, and author profiles for this publication at: <https://www.researchgate.net/publication/369093294>

Exhaustive in silico design and screening of novel antipsychotic compounds with improved pharmacodynamics and blood–brain barrier permeation properties

Article in *Journal of Biomolecular Structure and Dynamics* · March 2023

DOI: 10.1080/07391102.2023.2184179

CITATIONS

2

3 authors, including:



Yuri Porozov
HSE University

75 PUBLICATIONS 1,314 CITATIONS

[SEE PROFILE](#)

READS

128



Sergey Shityakov
University of Wuerzburg

165 PUBLICATIONS 1,841 CITATIONS

[SEE PROFILE](#)



Exhaustive *in silico* design and screening of novel antipsychotic compounds with improved pharmacodynamics and blood-brain barrier permeation properties

Radu Tamaian, Yuri Porozov & Sergey Shityakov

To cite this article: Radu Tamaian, Yuri Porozov & Sergey Shityakov (2023): Exhaustive *in silico* design and screening of novel antipsychotic compounds with improved pharmacodynamics and blood-brain barrier permeation properties, *Journal of Biomolecular Structure and Dynamics*, DOI: [10.1080/07391102.2023.2184179](https://doi.org/10.1080/07391102.2023.2184179)

To link to this article: <https://doi.org/10.1080/07391102.2023.2184179>



[View supplementary material](#)



Published online: 16 Mar 2023.



[Submit your article to this journal](#)



[View related articles](#)



[View Crossmark data](#)



Exhaustive *in silico* design and screening of novel antipsychotic compounds with improved pharmacodynamics and blood-brain barrier permeation properties

Radu Tamaian^a, Yuri Porozov^b and Sergey Shityakov^c

^aICSI Analytics, National Research and Development Institute for Cryogenics and Isotopic Technologies – ICSI Rm. Vâlcea, Râmnicu Vâlcea, Romania; ^bCenter of Bio- and Chemoinformatics, I.M. Sechenov First Moscow State Medical University, Moscow, Russia; ^cLaboratory of Chemoinformatics, Infochemistry Scientific Center, ITMO University, Saint-Petersburg, Russia

Communicated by Ramaswamy H. Sarma

ABSTRACT

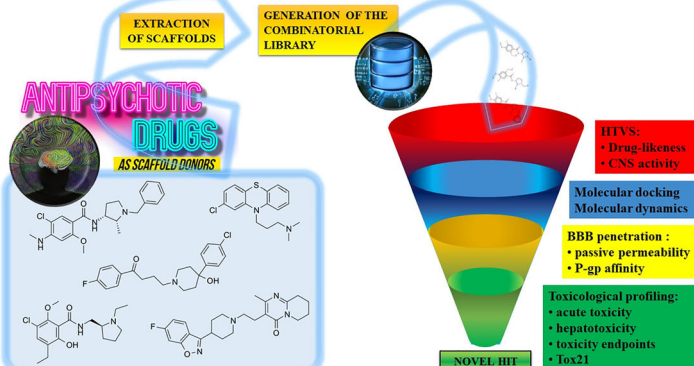
Antipsychotic drugs or neuroleptics are widely used in the treatment of psychosis as a manifestation of schizophrenia and bipolar disorder. However, their effectiveness largely depends on the blood-brain barrier (BBB) permeation (pharmacokinetics) and drug-receptor pharmacodynamics. Therefore, in this study, we developed and implemented the *in silico* pipeline to design novel compounds ($n=260$) as leads using the standard drug scaffolds with improved PK/PD properties from the standard scaffolds. As a result, the best candidates ($n=3$) were evaluated in molecular docking to interact with serotonin and dopamine receptors. Finally, haloperidol (HAL) derivative (1-(4-fluorophenyl)-4-(4-hydroxy-4-{4-[2-phenyl-1,3-thiazol-4-yl]methyl}phenyl)piperidin-1-yl)butan-1-one) was identified as a "magic shotgun" lead compound with better affinity to the 5-HT_{2A}, 5-HT_{1D}, D₂, D₃, and 5-HT_{1B} receptors than the control molecule. Additionally, this hit substance was predicted to possess similar BBB permeation properties and much lower toxicological profiles in comparison to HAL. Overall, the proposed rational drug design platform for novel antipsychotic drugs based on the BBB permeation and receptor binding might be an invaluable asset for a medicinal chemist or translational pharmacologist.

ARTICLE HISTORY

Received 15 September 2022
Accepted 18 February 2023

KEYWORDS

ADME-Tox; antipsychotics; blood-brain barrier permeation/penetration; CNS-active medications; dopamine and serotonin receptors; molecular dynamics; molecular docking; P-gp affinity; pharmacokinetics and pharmacodynamics



1. Introduction

Psychiatric disorders (PDs) have been associated with significant premature mortality, morbidity, financial burden, and negative socioeconomic impact. Even though several pharmacological approaches have been adopted to treat psychiatric disorders, it remains a difficult challenge to deal with (Aga et al., 2020; Harris, 2020). A significant percentage of patients still do not respond adequately to treatment schemes—leading to impaired functions and reduced quality

of life. Research studies on the distribution and determinants of PDs (mostly pinpoint to schizophrenia) have been extended worldwide in the last decade (Bai et al., 2020; Jongsma et al., 2019; McCutcheon et al., 2020; Moreno-Küstner et al., 2018; Mwesiga et al., 2020; Subramaniam et al., 2021; Wang et al., 2016). These new data may provide new insights into the determinants of the heterogeneity in the prevalence of mental disorders among and within different populations, supporting both service planning and

understanding of the neurophysiology of psychosis and (neurophysiological) biomarkers of psychosis risks for better planning of an effective public mental health strategy and a more adequate response (de Bartolomeis et al., 2022; Wang et al., 2022). The lifetime prevalence of PDs varies across different geographic regions, between genders, different ethnicities, and social categories, ultimately indicating that the main priority of clinicians around the world is to provide adequate clinical treatment, out-of-hospital management of patients, and mental health-care strategies (Aga et al., 2020; Cobaugh et al., 2007; Jongsma et al., 2019; Moreno-Küstner et al., 2018; Subramaniam et al., 2021; Wang et al., 2022; Yang et al., 2021), recently adapted to the COVID-19 pandemic context in many countries (Eugene et al., 2021; Haddad et al., 2022; Heron et al., 2022; Mwesiga et al., 2021; Oka et al., 2021; Taquet et al., 2021; Jayaraj et al., 2022). Antipsychotic drugs are a type of psychiatric medication typically approved for the treatment of PDs (Aga et al., 2020; de Bartolomeis et al., 2022; Harris, 2020) and can be also used to deal with depressive disorders (Cantù et al., 2021; Simons et al., 2017; Wang & Si, 2013), and bipolar disorder (Bai et al., 2020; Edwards & Smith, 2009; Hu et al., 2022) or non-psychiatric health issues. In this respect, chlorpromazine is an approved medicine for the treatment of persistent and intractable hiccups (Polito & Fellows, 2017), while olanzapine is known for its efficacy in palliative care of chemotherapy-induced nausea and vomiting (Roffman & Pirl, 2003; Saudemont et al., 2020).

Despite their clinical benefits, antipsychotics have many adverse effects and may affect differently various categories of patients and are notorious for their associations with toxicity concerns and a plethora of side effects localized at the level of the central nervous system (CNS) and neuromuscular system (Barnes & Edwards, 1993), respectively at the level of other physiological systems (Edwards & Barnes, 1993). From a patient-centric perspective (Edwards & Smith, 2009; Harris, 2020; Stroup & Gray, 2018), the most common adverse effects of antipsychotics can be categorized, in terms of tolerability, as common/tolerable and unpleasant issues, followed by painful issues, disfiguring medication-induced conditions, and, even further development of life-threatening disorders (Table 1).

Currently, it is widely accepted that major PDs, including here schizophrenia, have pluralistic origins, involving dysregulation of multiple molecular signalling pathways (de Bartolomeis et al., 2022; Kim & Stahl, 2010; McCutcheon et al., 2020; McGowan & Reynolds, 2020), with additional genetic and epigenetic components (de Bartolomeis et al., 2022; Ganapathiraju et al., 2016; Roth et al., 2004), and under continuous pressure of gene-environment interactions (McGowan & Reynolds, 2020; Pence et al., 2022; Roth et al., 2004). Consequently, the most effective treatment schemes have extremely complex pharmacology whilst single molecular targets strategies unsurprisingly failed (Kim & Stahl, 2010; Roth et al., 2004). Therefore, the rational design of "selectively non-selective drugs" (the so-called "magic shotguns") (Roth et al., 2004) able to interact with multiple molecular targets became a true paradigm shift that can lead to the development of safer and/or, and more effective drugs for PDs with multiple molecular signalling pathways (de Bartolomeis et al., 2022; Kim & Stahl, 2010; Kondej et al., 2018; Roth et al., 2004).

This paper refers to a computational work for the rational design of novel and safer antipsychotic drug prototypes, inhibitors of dopamine (DA) and serotonin (5-hydroxytryptamine, abbreviated as 5-HT) receptors—key targets in molecular signalling pathways of schizophrenia, major PDs and some others CNS disorders (Burns, 2001; Harris, 2020; Kondej et al., 2018; McCutcheon et al., 2020; McGowan & Reynolds, 2020; Roth et al., 2004).

DA receptors are part of the G protein-coupled receptor (GPCR) superfamily and include five genes that encode different receptors, divided into two pharmacological families: D₁-like and D₂-like receptors (Deng & Dean, 2013; Kim & Stahl, 2010). The D₁-like family receptors (D₁ and D₅ receptors—predominantly found postsynaptic) are coupled to the G_{sα}, which subsequently activates adenylyl cyclase, increasing the intracellular concentration of cAMP (D₁ is additionally coupled to G_{olf}). D₂-like family receptors (D₂, D₃, and D₄ receptors—located both at postsynaptic and presynaptic levels on dopaminergic target neurons; and presynaptic as autoreceptors on dopamine neurons) are coupled to the G_{iα}, which directly inhibits the formation of cAMP by inhibition of adenylyl cyclase. DRD2 gene alternative splicing results in three transcript variants of D₂ receptors, from which D_{2LH} (long form) has the canonical sequence, functioning as a classic postsynaptic receptor.

Table 1. The most common adverse effects of antipsychotics from a patient tolerability perspective.

Category	Adverse effect	References
Tolerable issues	Mild sedation	(Barnes & Edwards, 1993; Eugene et al., 2021; Harris, 2020; Seale et al., 2007)
Unpleasant issues	Xerostomia (dry mouth)	(Aga et al., 2020; Barnes & Edwards, 1993; Harris, 2020; Wang et al., 2016)
	Urinary incontinence	(Aga et al., 2020; Edwards & Barnes, 1993; Edwards & Smith, 2009)
	Constipation	(Aga et al., 2020; Bai et al., 2020; Edwards & Smith, 2009; Harris, 2020)
Unpleasant escalating to painful issues	Sexual dysfunctions ^a	(Aga et al., 2020; Edwards & Barnes, 1993; Edwards & Smith, 2009; Harris, 2020)
Painful issues	Acute akathisia	(Barnes & Edwards, 1993; Edwards & Smith, 2009; Harris, 2020; Wang et al., 2016)
Disfiguring conditions	Acute dystonic reactions	(Aga et al., 2020; Barnes & Edwards, 1993; Cobaugh et al., 2007; Harris, 2020)
	Tardive dyskinesia	(Barnes & Edwards, 1993; Cobaugh et al., 2007; Harris, 2020; Simons et al., 2017)
	Obesity	(Edwards & Barnes, 1993; Edwards & Smith, 2009; Harris, 2020; Subramaniam et al., 2021)
Life-threatening disorders	Dyslipidemia ^b	(Harris, 2020; Stroup & Gray, 2018; Yang et al., 2021)
	Myocarditis	(De las Cuevas et al., 2021; Edwards & Smith, 2009; Harris, 2020)
	Agranulocytosis ^c	(Aga et al., 2020; Cobaugh et al., 2007; Edwards & Smith, 2009; Harris, 2020)

^aIn terms of loss of sexual interest and drive (in both men and women) and male sexual dysfunction.

^bAn important risk factor for cardiovascular diseases.

^cVery high-risk of severe infections due to the weakened immune system.

5-HT receptors include members from six families of G protein-coupled receptors (5-HT₁, 5-HT₂, and 5-HT₄ – 5-HT₇ receptors) and one ligand-gated Na⁺ and K⁺ cation channel (5-HT₃ receptor) (Kim & Stahl, 2010; McGowan & Reynolds, 2020). 5-HT₁ and 5-HT₅ receptors are G_i/G_o-protein coupled, 5-HT₂ receptors are G_q/G11 protein-coupled, and meanwhile, 5-HT₄, 5-HT₆ and 5-HT₇ receptors are G_s-protein coupled.

2. Materials and methods

Briefly, a multi-target strategy (Kondej et al., 2018; Roth et al., 2004; Zhang et al., 2017) was used for *in silico* rational design of new antipsychotic drug prototypes as inhibitors of DA and 5-HT receptors. Hence, it was generated a virtual combinatorial library (Liu et al., 2017) based on molecular scaffolds from a selected list of antipsychotic compounds, including here scaffolds and additional substructures from some worldwide approved drugs, a perspective approach in drug discovery (Ertl, 2021; Harel & Radinsky, 2018; Taylor et al., 2017). Virtual compounds included in the combinatorial library were massively filtered using ADME-Tox predictors—cheminformatics tools designed to evaluate absorption, distribution, metabolism, excretion (ADME), and toxicity (ADME-Tox)—for improved pharmacokinetics and capability of direct activity at the CNS level by penetration of the blood-brain barrier (BBB) (Lipinski, 2005). By linking protein-ligand docking (P-LD) with molecular dynamics (MDs) (Sivakumar et al., 2020) were evaluated the spatial orientation, binding energy (BA) of the safer drug candidates in the selected target's active sites, and stability of the protein–ligand complex to identify the most potent inhibitors, able to form a stable complex with molecular targets.

2.1. Generation of a combinatorial library based on scaffolds from known inhibitors of DA and 5-HT receptors

2.1.1. Identification of scaffold donors based on knowledge of their molecular targets

Scaffold donors for the generation of the combinatorial library were selected with the help of The IUPHAR/BPS Guide to PHARMACOLOGY, Release Version 2021.4 (14th of December, 2021) (<https://www.guidetopharmacology.org/>) (NC-IUPHAR, 2022). As a quasi-empirical selection criterion was imposed that inhibitors of DA and 5-HT receptors belong to the different types of antipsychotics, including here approved drugs and experimental molecules. Additionally, it was requested that inhibitors of DA and 5-HT receptors have at least one of the DA and 5-HT receptors as molecular targets and to be able to be the antagonist of the aforementioned receptors, respectively able to interact with multiple molecular targets. Further, a cross-check with the help of The Research Collaboratory for Structural Bioinformatics Protein Data Bank (RCSB PDB) site (<http://www.rcsb.org/>) (Berman, 2003; Berman et al., 2000; Burley et al., 2021; 2022) was performed in order to identify the best crystal structures of targets for P-LD and MDs—a final selection criterion.

2.1.2. Generation of the combinatorial library

For the construction of the combinatorial library was used SmiLib v2.0 rc2 (Schüller et al., 2003), software that operates with three classes of enhanced SMILES strings (Weininger, 1988) as input data: scaffold molecules (Markush structures of molecules that contain the sites of variability or R-groups), building blocks (BBs—small Markush structures) and linkers (connectors between scaffolds and BBs). Due to the restrictions regarding the upper limits of molecular weight (MW) of drug-like compounds, in accordance with Lipinski's rule of five (RO5) (Lipinski, 2016; Lipinski et al., 2001; 2012), respectively Egan's rule (Egan et al., 2000) and Veber's rule (Veber et al., 2002) for a good oral bioavailability, a set of three scaffolds with reduced MW with up to two variability sites were built for each of the selected antipsychotic compounds. A set of seven BBs, part of a previously developed larger library (Tamaian et al., 2010), were used for the second class of enhanced SMILES strings required as input data for SmiLib v2.0 rc2 software (Figure 1). In this particular study was used a “pseudo linker” or empty linker was due to the aforementioned MW restrictions. MarvinSketch was used for drawing, displaying, and two-dimensional (2D) optimization, generations of enhanced SMILES strings, and graphical processing of 2D images made for all Markush structures, MarvinSketch version 19.9.0, ChemAxon (<https://chemaxon.com/>).

2.2. Virtual screening of combinatorial library

High-throughput Virtual screening VS has emerged as positive feedback to the pressure raised by combinatorial chemistry and the expensive high-throughput screening (HTS) of small-molecules drug candidates (Lipinski, 2005). *In silico* evaluation of a large combinatorial library (including scaffold donors as a control) via an VS approach was used to identify the best drug candidates in terms of improved pharmacokinetics and CNS activity.

Prediction of the ADME-Tox properties was performed with FAF-Drugs4 software (Lagorce et al., 2017). The combinatorial library (generated as SDF file format with SmiLib v2.0 rc2) was formatted in accordance with the FAF-Drugs4 requirements using the Bank Formatter submodule (Lagorce et al., 2015). Estimation of the octanol-water partition coefficient (LogP), the entry point for derived ADME-Tox descriptors, was made using the XLOGP3 method (Cheng et al., 2007), an additive model based on previously experimentally gained knowledge. In this VS setup was used an extended set of build-in filters for evaluations of drug-likeness and pharmacokinetics predictors. The *Drug-Like Soft* filter implemented in FAF-Drugs4 (Lagorce et al., 2017) was developed based on several articles related to the physico-chemical properties of drugs (Irwin & Shoichet, 2005; Lipinski, 2005; Lipinski et al., 2001; Oprea, 2000; Oprea et al., 2001) combined with an in-house statistical analysis (Lagorce et al., 2015) of approved drugs included in the e-Drugs3D library (Pihan et al., 2012) (Table 2).

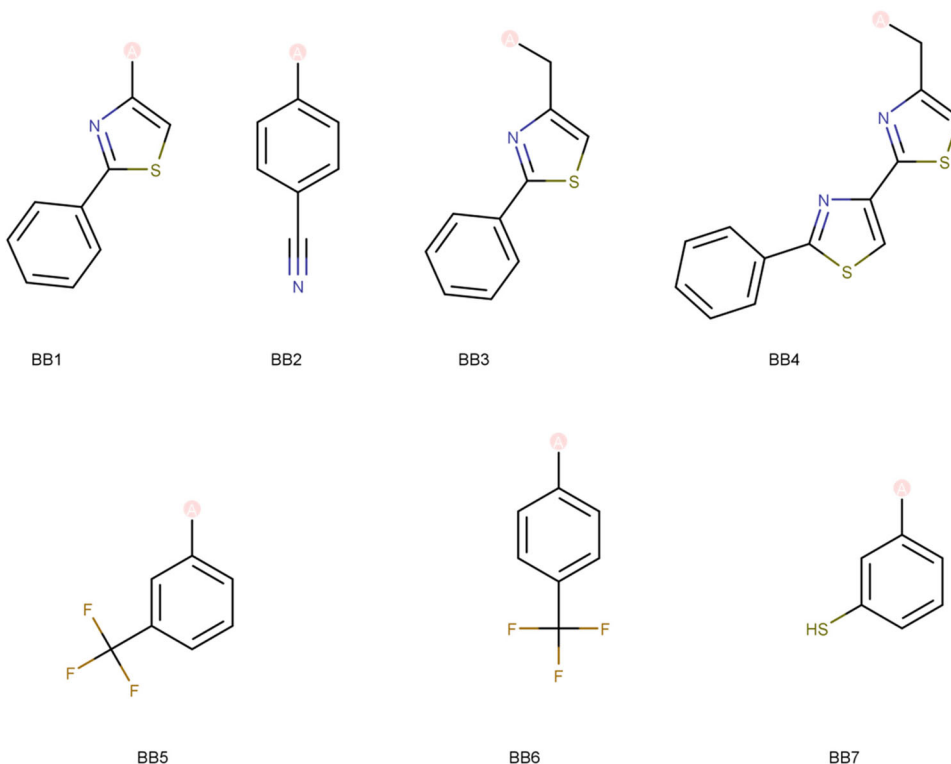


Figure 1. 2D depiction of BBs. ® represents the attachment sites of BBs to the scaffolds.

Table 2. Threshold values of the computed parameters with the *Drug-Like Soft* filter.

Parameter (S.I. Units)	Abbreviation	Threshold values
Molecular weight (Da)	MW	100 to 600
Octanol-water partition coefficient	LogP	-3 to 6
Hydrogen bond acceptors ^a	HBA	≤12
Hydrogen bond donors ^b	HBD	≤7
Topological polar surface area (Å ²) ^c	tPSA	≤180
Number of rotatable bonds ^d	RotBs	≤11
Number of rigid bonds	RigBs	≤30
Number of smallest set of smallest rings	SSSR	≤6
Size of the biggest system ring	SBSR	≤18
Number of the carbon atoms	CARBs	3 to 35
Number of heteroatoms ^e	HETs	1 to 15
Ratio between carbon atoms and heteroatoms	Ratio H/C	0.1 to 1.1
Number of charged groups	CGs	≤4
Formal total charge of the compound	FTC	-4 to 4
Maximum number of violations of RO5	RO5 violations	2
Veber's rule for oral bioavailability	VeberBioAv	tPSA < 140 Å ² or RotBs < 10
Egan's rule for oral bioavailability	EganBioAv	tPSA < 131.6 Å ² or LogP < 5.88

^aSum of all oxygen and nitrogen atoms (according to RO5).

^bSum of all -OH and -NH groups (according to RO5).

^cSummation of tabulated surface contributions of polar fragments (including the bonding patterns of atoms) (Ertl et al., 2000).

^dNumber of any single non-ring bond, bounded to non-terminal heavy atom (the amide C–N bonds are not considered because of their high rotational energy barrier (Veber et al., 2002)).

^eNumber of non-carbon atoms (hydrogen atoms are not included).

Main pharmacokinetics predictors implemented in the FAF-Drugs4 software and used in this experimental setup include the detection of:

- non-peptidic inhibitors of protein-protein interactions (iPPIs) by using a decision tree based on the review of scientific literature (Sperandio et al., 2010) and a machine-learning implementation (Reynès et al., 2010), which was developed with the help of two Dragon descriptors (Ui and RDF070m) (Todeschini & Consonni, 2008);
- undesirable moieties and substructures (UMSs) based on an extended collection of scientific literature data (Enoch et al.,

2011; Blagg, 2010; Benigni & Bossa, 2011; Stepan et al., 2011; Bruns & Watson, 2012; Rishton, 2003; Cumming et al., 2013; Singh et al., 2009; Horvath et al., 2014; Smith, 2011);

- covalent inhibitors using a data collection of covalent modifiers (Potashman & Duggan, 2009) and a high throughput kinetic profiling for skin sensitization (Roberts & Natsch, 2009);
- Pan-Assay Interference Compounds (PAINS) by three detection filters (filter A with over 150 analogs, filter B with 15 to 149 analogs, and filter C with 1 to 14 analogs) of compounds that act as frequent hitters in biochemical HTS (Baell & Holloway, 2010; Mok et al., 2013).

Moreover, customized filters based on the estimation of phospholipidosis induction (Phl) (Przybylak et al., 2014), molecular complexity (Fsp3 rule, referring to the number of sp^3 hybridized carbons/total carbon count) (Lovering et al., 2009), and rules developed by pharmaceutical companies were used for additional drug-likeness and safety profiling: GlaxoSmithKline's 4/400 rule (GSK 4/400) (Gleeson, 2008), Pfizer's "Rule of 3/75" (Ro3.75) (Hughes et al., 2008), respectively Eli Lilly and Company's rules for identification of "potentially reactive or promiscuous compounds" (MedChem) (Bruns & Watson, 2012). MedChem rules were used with the regular settings implemented in the FAF-Drugs4 software (100-demerit cutoff).

The activity at the CNS level was predicted using the threshold values of five parameters (Jeffrey & Summerfield, 2010) implemented as a CNS filter in FAF-Drugs4: MW (135 to 582 Da), LogP (-0.2 to 6.1), HBA (≤ 5), HBD (≤ 3) and tPSA (3 to 118 Å²). The activity at the CNS level was used as an eliminatory condition for virtual derivatives unable to fit within the threshold values imposed for all investigated parameters. This set of filters allows for predicting the passive BBB permeability (Lipinski, 2005).

2.3. Virtual screening of the safest drug candidates

VS runs were carried out only on the safest drug candidates with expected activity at the CNS level (based only on the output of the basic CNS filters implemented in FAF-Drugs4). Molecular docking was performed to identify the spatial orientation and best binders of the safest drug candidates, followed by molecular dynamics simulations to evaluate, in time, the stability of the predicted protein-ligand complexes and permeation phenomena at the level of BBB. Finally, more advanced toxicity predictors (in terms of necessary computing power, time management and predicted toxicity endpoints) were used to individually re-evaluate, the safety profiles of the safest drug candidates for the detection of possible additional health risks.

2.3.1. Protein-ligand docking (P-LD)

Separate P-LD runs were carried out for each identified molecular target with AutoDock Vina v.1.2.0 (Trott & Olson, 2010), using PyRx—Python Prescription v.0.9.7 (Dallakyan & Olson, 2015) as a control interface. AutoDock Vina automatically calculates the grid maps and finally clusters the docking results in a transparent way for an improved user experience. Experimentally determined crystal structures of identified targets (PDB ID: 4IAR, 7E32, 6A93, 6CM4, 3PBL, and 5WIU) were extracted from the RCSB PDB site (<http://www.rcsb.org/>) (Berman, 2003; Berman et al., 2000; Burley et al., 2021; 2022). MarvinSketch was used for drawing, displaying, and 3D optimization and generations of ligands files (Tripos MOL2 file format) required for docking, MarvinSketch version 19.9.0, ChemAxon (<https://chemaxon.com/>). All P-LD runs were carried out in a search space lower than 27,000 Å³ (around the binding site of co-crystallized ligands from the X-ray 3D structure of molecular targets—as recommended by the

software developers (Trott & Olson, 2010)) and the value of exhaustiveness was set to 200 to improve the accuracy of docking process (the default value of exhaustiveness is set to 8 in PyRx v.0.9.7). Co-crystallized ligands of each identified molecular target were re-docked as a control/reference ligands of corresponding P-LD runs. Supplementary, all scaffold donors were included in each docking run for comparison purposes.

Molegro Molecular Viewer 2.5 (Molegro—A CLC bio company, Århus, Denmark; currently acquired by QIAGEN Digital Insights, Århus, Denmark) was used for post-docking operations, such as: re-ranking of the best poses, data extraction, high-resolution renderings of the best poses of protein-ligand complexes. The re-ranking procedure involves the use of a complex scoring function (Thomsen & Christensen, 2006), based on a previously introduced piecewise linear potential (PLP) (Gehlhaar et al., 1995). The scoring function used for re-ranking of the best poses includes, besides docking scoring function descriptors, an sp^2 - sp^2 torsion term and a Lennard-Jones 12-6 potential (LJ12-6) (Morris et al., 1998).

2.3.2. Molecular dynamics (MD) simulation

The POPC:POPE:Cholesterol (100:100:50) bilayer was built using the CHARMM-GUI pipeline designed to generate membrane-bound protein structures (Jo et al., 2008). To properly orient the protein structure in the Z direction, we aligned the first principal axis along the Z-axis according to the CHARMM-GUI protocol. The system was solvated according to the lipid hydration numbers available elsewhere (Kučerka et al., 2005). All MD simulations were performed using the AMBER 20 package (Salomon-Ferrer et al., 2013) with the lipid14, ff99SB, and GAFF force fields for the membrane, protein, and ligand, respectively. The antechamber module of AmberTools was employed to calculate the AM1-BCC charges for the ligands. Cl⁻ or Na⁺ ions were added to neutralize the solvated membrane-protein-ligand system. Long-range electrostatic interactions were modelled via the particle-mesh Ewald method. The SHAKE algorithm (Ryckaert et al., 1977) was applied to constrain the length of covalent bonds, including the hydrogen atoms. The standard MD protocol included the minimization (10000 cycles), heating (15 ps), equilibration (5 ns) of periodic box dimensions, and production (200 ns) with constant pressure. Finally, the linear interaction energy method was implemented to calculate ΔG_{lie} using the following equation:

$$\Delta G_{lie} = \alpha \cdot \Delta E_{vdW} + \beta \cdot \Delta E_{elec}, \quad (1)$$

where ΔE_{vdW} is the difference between the van der Walls terms for ligand/protein and ligand/water interactions; and ΔE_{elec} is the difference between the electrostatic terms for ligand/protein and ligand/water interactions with default scaling factors ($\alpha = 0.18$ and $\beta = 0.5$).

2.3.3. Permeation phenomena at the level of the BBB

The BBB permeation of each investigated compound (selected VDs and their scaffold donors) was assessed by different approaches: 1) calculation of the logBB (logarithmic

ratio between the concentration of a compound in the brain and in the blood)—the most common parameter related to the passive BBB permeability, 2) computational assessment of the probability of the passive BBB permeability based on a substructure pattern recognition (sSPR) method, 3) evaluation of the CNS permeability by computation of the BBB permeability-surface area product (LogPS), and 4) prediction of the affinity for P-glycoprotein (P-gp—membrane transport protein located inclusively at the level of the brain microvascular endothelial cells). P-gp determines the uptake and efflux of xenobiotics at the level of BBB and many anti-psychotic drugs act as inhibitors of P-gp, and subsequently can influence plasma and brain concentrations of various xenobiotics which are P-gp substrates—including here other antipsychotics (Aga et al., 2020; De Leon, 2009; Moons et al., 2011). Furthermore, the xenobiotics with affinity to the various membrane transport proteins are known exceptions to the physicochemical-based filters (Lipinski, 2005), inclusively the aforementioned CNS filter (Jeffrey & Summerfield, 2010) implemented in the FAF-Drugs4 software (Lagorce et al., 2017) and used for VS of the complete combinatorial library.

The logBB parameters were calculated with Clark (Clark, 1999), and Rishton (Rishton et al., 2006) equations using ClogP (Leo, 1993) and tPSA as predictors:

$$\text{logBB}_{\text{Clark}} = 0.152 \cdot \text{ClogP} - 0.0148 \cdot \text{tPSA} + 0.139, \quad (2)$$

$$\text{logBB}_{\text{Rishton}} = 0.155 \cdot \text{ClogP} - 0.01 \cdot \text{tPSA} + 0.164. \quad (3)$$

Molecules readily permeable through BBB were filtered by logBB threshold of 0.3 proposed by Kunwittaya et al. during the model development for BBB permeability prediction on the dataset of compounds with known logBB values (Kunwittaya et al., 2013).

The admetSAR software (Cheng et al., 2012) was used to predict the probability of passive BBB permeability (BBB_{P-Prob}) and assessment of P-gp affinity for substrates and inhibitors. All the aforementioned predictors use combined qualitative

classification models, instead of simple binary output, developed with the help of SVM (support vector machine) classification algorithm and the in-house sSPR method (Shen et al., 2010). The sSPR method includes the 3D conformations for some descriptors (e.g.: for BBB_{P-Prob} the molecular substructure pattern fingerprints were developed based on predefined substructure pattern dictionaries freely available from the Open Babel chemical toolbox—FP4 and MACCS) (Shen et al., 2010). The robustness of BBB_{P-Prob} and P-gp affinity models was validated based on 5-fold cross-validation. For the BBB_{P-Prob} model, the complete dataset includes 1839 compounds (1438 compounds able to penetrate the BBB and 401 compounds unable to permeate via BBB) from previous work (Adenot & Lahana, 2004). The area under the receiver operating characteristic curve (AUC) is 0.952 for the BBB_{P-Prob} model. The P-gp substrate probability model implemented in admetSAR is built using a 332 compounds dataset (206 P-gp substrates and 126 Pg-p non-substrates) collected from previous work (Wang et al., 2011). The AUC is 0.768 for the P-gp substrate probability model. P-gp inhibitor probability was computed with the admetSAR software using two different models: P-gp inhibitor I and P-gp inhibitor II. The P-gp inhibitor I model has a 1273 compounds dataset (797 Pg-p inhibitors and 476 Pg-p non-inhibitors) (Chen et al., 2011) whilst the P-gp inhibitor II model dataset includes 1275 compounds (666 P-gp inhibitors and 609 P-gp non-inhibitors) (Broccatelli et al., 2011). The AUC is 0.853 for the P-gp inhibitor I model, respectively 0.922 for the P-gp inhibitor II model. To be mentioned that from all the aforementioned models implemented in admetSAR, only the P-gp inhibitor II model contains HTS data (Cheng et al., 2012).

The pkCSM web-server (Pires et al., 2015) was used for the evaluation of LogPS and P-gp affinity. LogPS is a less commonly used *in silico* descriptor, but perhaps a more precise and invasive *in vivo* method (e.g. *in situ* carotid perfusion) for the evaluation of the CNS permeability because it

Table 3. Correlations between identified scaffold donors and their molecular targets in humans.

Scaffold donors vs. Targets (RCSB PDB ID)	CHL	RIS	HAL	EMO	ETI
	References				
5-HT _{1B} receptor (4IAR)	ND	PT (Lesage et al., 1998; Schotte et al., 1996; Shahid et al., 2009)	ND	ND	ND
5-HT _{1D} receptor (7E32)	ND	PT (Leysen et al., 1996; Schotte et al., 1996)	NPT (Schotte et al., 1996)	ND	ND
5-HT _{2A} receptor (6A93)	PT (Kroeze et al., 2003)	PT (Kongsamut et al., 2002; Kroeze et al., 2003; Schotte et al., 1996)	PT (Kroeze et al., 2003; Millan et al., 1999; Schotte et al., 1996; Shahid et al., 2009; Vanover et al., 2004)	ND	ND
D ₂ receptor (6CM4)	ST (Freedman et al., 1994; Sokoloff et al., 1992)	PT (Arnt & Skarsfeldt, 1998)	PT (Freedman et al., 1994; MacKenzie et al., 1994; Mierau et al., 1995; Sokoloff et al., 1992; Tice et al., 1994)	ND	NPT (MacKenzie et al., 1994; Tang et al., 1994)
D ₃ receptor (3PBL)	NPT (Freedman et al., 1994; Sokoloff et al., 1992)	NPT (Millan et al., 1995)	PT (Freedman et al., 1994; Shahid et al., 2009; Sokoloff et al., 1992; Tice et al., 1994)	NPT (MacKenzie et al., 1994; Tang et al., 1994)	NPT (MacKenzie et al., 1994; Tang et al., 1994)
D ₄ receptor (5WIU)	NPT (Lahti et al., 1993)	ND	PT (Lahti et al., 1993; Shahid et al., 2009; Tice et al., 1994)	NPT (Seeman et al., 1993)	NPT (Durcan et al., 1995)

PT: primary target in humans; NPT: not a primary target in humans; ND: no data; target classification is in accordance with The IUPHAR/BPS Guide to PHARMACOLOGY, Release Version 2021.4.

eliminates the effect of serum binding of the investigated xenobiotics. The pkCSM predictors were developed with the help of machine learning approaches utilizing distance-based graph signatures. The predictive model for LogPS was built using a 153 compounds dataset (detailed experimental measurements, mostly from rats) (Suenderhauf et al., 2012) and the robustness of the LogPS model was validated via 10-fold cross-validation (Yan et al., 2013). The pkCSM novel approach exhibits similar performance and/or a lower standard error for the case of the BBB permeability dataset than the original work, which is using machine learning paradigms (decision tree induction) (Suenderhauf et al., 2012). For estimation of the P-gp affinity, the pkCSM web-server uses the same datasets as the admetSAR software (Cheng et al., 2012); respectively the

P-gp substrate probability model has a 332 compounds dataset (Wang et al., 2011), the P-gp inhibitor I model have 1273 compounds dataset (Chen et al., 2011) and the P-gp inhibitor II model has a 1275 compounds dataset (Broccatelli et al., 2011). The performance for the classification of the P-gp substrate probability model between the pkCSM web-server ($AUC = 0.814$) and the admetSAR software ($AUC = 0.768$) is considered to be similar. However, the pkCSM web-server surpasses the admetSAR software for both of the P-gp inhibitor models having a statistically significant performance difference calculated using a nonparametric Wilcoxon statistic method (Hanley & McNeil, 1982) with a threshold of ≤ 0.05 for significance. In the case of the pkCSM web-server, the AUC is 0.906 for the P-gp inhibitor I model ($AUC = 0.853$ for the admetSAR

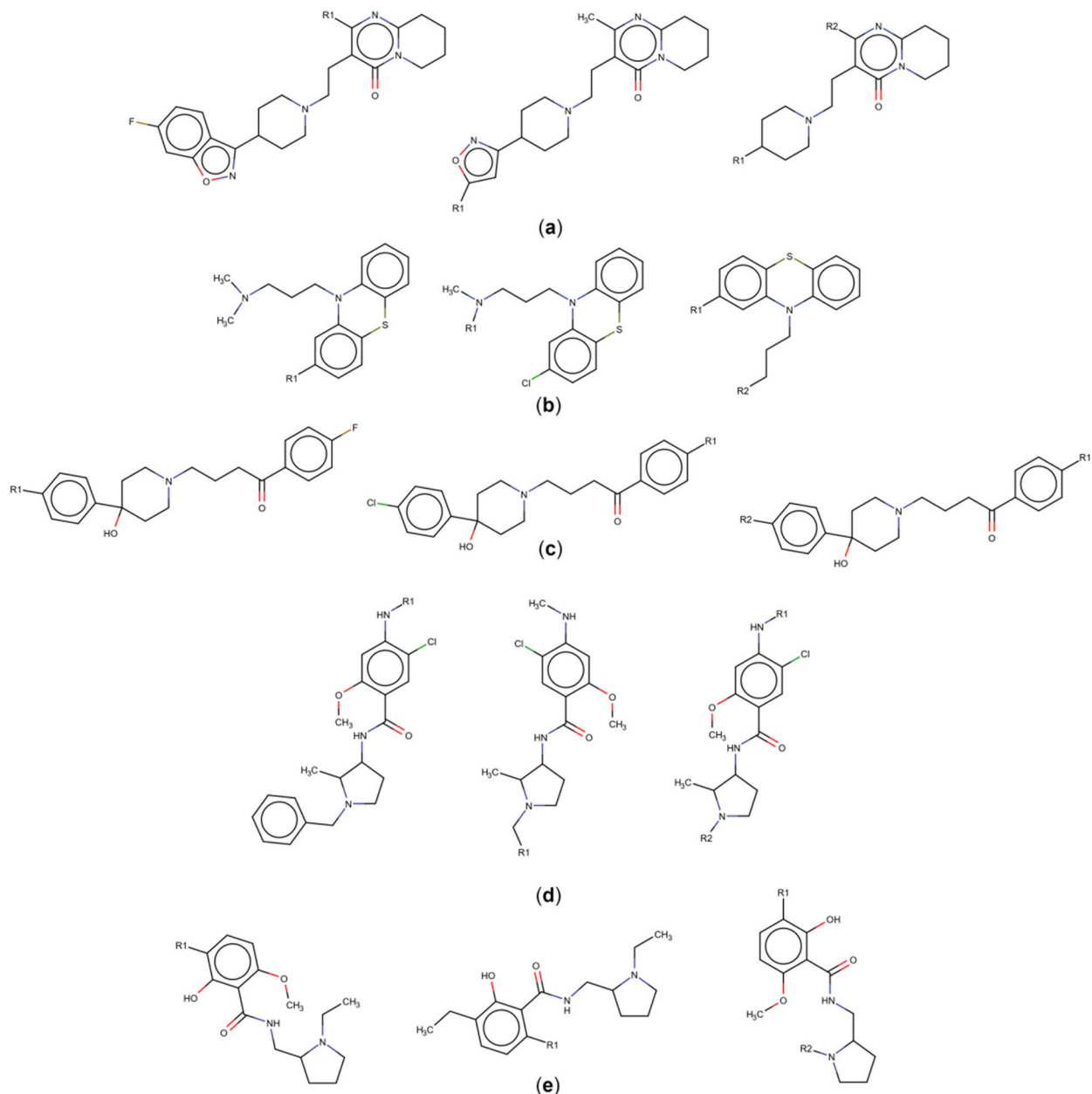


Figure 2. 2D depiction of scaffolds designed by reduction of MW. (a) Scaffolds based on CHL's backbone; (b) Scaffolds based on RIS's backbone; (c) Scaffolds based on HAL's backbone; (d) Scaffolds based on EMO's backbone; (e) Scaffolds based on ETI's backbone.

Table 4. Computed parameters with the *Drug-Like Soft* filter and CNS filter for scaffold donors.

Parameter (S.I. Units)	CHL	RIS	HAL	EMO	ETI
MW (Da)	318.86	410.48	375.86	387.90	306.40
LogP	5.41	2.72	4.30	3.94	2.11
HBA	<u>2</u>	6	3	5	5
HBD	0	0	1	2	2
tPSA (\AA^2)	32.98	65.36	41.74	54.80	63.00
RotBs	4	4	6	6	6
RigBs	16	28	19	19	13
SSSR	1	3	3	3	2
SBSR	14	10	6	6	6
CARBs	17	23	21	21	17
HETs	4	7	5	6	5
Ratio H/C	0.24	0.30	0.24	0.29	0.29
CGs	1	1	1	1	1
FTC	1	1	1	1	1
RO5 violations	1	0	0	0	0
VeberBioAv	Good	Good	Good	Good	Good
EganBioAv	Good	Good	Good	Good	Good

Underline value: violation of RO5 ($\text{LogP} \leq 5$); **bold and italicized value**: value is outside of the threshold considered for activity at the CNS level via passive permeation ($\text{HBA} \leq 5$).

Table 5. Computed pharmacokinetics predictors and toxicology profilers for scaffold donors.

Computed predictor	CHL	RIS	HAL	EMO	ETI
iPPIs	Yes	No	Yes	Yes	Yes
Number of UMSs	¹ _{LRH}	¹ _{LRH-F}	² _{LRH, LRH-F}	¹ _{LRH}	0
Covalent inhibitors	No	No	No	No	No
PAINS (filter A)	0	0	0	0	0
PAINS (filter B)	0	0	0	0	0
PAINS (filter C)	0	0	0	0	0
PhI	Yes	No	Yes	No	No
Fsp3	0.29	0.52	0.38	0.38	0.59
GSK 4/400 ^{OBS}	Good	Good	Good	Good	Good
Ro3.75	Bad	Warning	Bad	Bad	Warning
MedChem	Pass	Pass	Pass	Pass	Pass

^{LRH}: substructure rule “Low_Risk_halogenure” (Chlorine, Bromine and Iodine atoms are counted all together) – rejection threshold is 5 atoms; ^{LRH-F}: substructure rule “Low_Risk_halogenure_F” (only Fluorine atoms are counted) – rejection threshold is 7 atoms; ^{OBS}: according with this rule, compounds with $\text{LogP} > 4$ and MW > 400 Da have a less favourable safety profile (check Table 4 for computed values).

software), respectively 0.948 for the P-gp inhibitor II model (AUC = 0.922 for the admetSAR software).

2.3.4. Individual toxicological profiling of the safest drug candidates

ProTox-II web-server (Banerjee et al., 2018) was used for individual toxicological profiling of the safest drug candidates. ProTox-II incorporates a set of trained models (molecular similarity, pharmacophores, fragment propensities and machine-learning models) built on data from *in vitro* assays and *in vivo* cases for some critical toxicity endpoints, such as acute toxicity, organ toxicity, toxicity endpoints, and the adverse outcomes pathways (Tox21) (Roper & Tanguay, 2020). The trained models were developed for acute toxicity (expressed as lethal dose for oral toxicity—LD_{50,oral}, in accordance with the globally harmonized system of classification and labelling of hazardous chemicals), hepatotoxicity, three toxicology endpoints (carcinogenicity, immunotoxicity, and mutagenicity), respectively nuclear receptor signalling pathways and stress response pathways for evaluation of Tox21.

Table 6. Computed parameters with the *Drug-Like Soft* filter and CNS filter for the best drug candidates.

Parameter (S.I. Units)	HAL_1.1_3_3_3	ETI_3.1_1_57_57	ETI_3.1_3_59_59
MW (Da)	514.65	435.58	449.61
LogP	<u>6.67</u>	5.51	5.80
HBA	<u>4</u>	<u>5</u>	<u>5</u>
HBD	1	2	2
tPSA (\AA^2)	82.8	94.9	94.9
RotBs	9	7	8
RigBs	30	24	24
SSSR	5	4	4
SBSR	6	6	6
CARBs	31	25	26
HETs	6	6	6
Ratio H/C	0.19	0.24	0.23
CGs	1	1	1
FTC	1	1	1
RO5 violations	2	1	1
VeberBioAv	Good	Good	Good
EganBioAv	Good	Good	Good

Bolded parameters: parameters that are considered not only by the *Drug-Like Soft* filter, but also by the CNS filter (no violations of threshold values for CNS filter were detected); underline values: violations of RO5 ($\text{LogP} \leq 5$, respectively MW ≤ 500 Da).

Table 7. Computed pharmacokinetics predictors and toxicology profilers for the best drug candidates.

Computed predictor	HAL_1.1_3_3_3	ETI_3.1_1_57_57	ETI_3.1_3_59_59
iPPIs	No	No	No
Number of UMSs	¹ _{LRH-F}	0	0
Covalent inhibitors	No	No	No
PAINS (filter A)	0	0	0
PAINS (filter B)	0	0	0
PAINS (filter C)	0	0	0
PhI	No	No	No
Fsp3	0.29	0.36	0.38
GSK 4/400 ^{OBS}	Bad	Bad	Bad
Ro3.75	Warning	Warning	Warning
MedChem	Pass	Pass	Pass

^{LRH-F}: substructure rule “Low_Risk_halogenure_F” (only Fluorine atoms are counted) – rejection threshold is 7 atoms; ^{OBS}: according to this rule, compounds with $\text{LogP} > 4$ and MW > 400 Da have a less favourable safety profile (check Table 6 for previously computed values).

3. Results and discussion

3.1. Generation of combinatorial library

3.1.1. Identification of scaffold donors based on knowledge of their molecular targets

A total of five scaffold donors, belonging to four categories of compounds, were identified for the generation of the combinatorial library by cross-checking The IUPHAR/BPS Guide to PHARMACOLOGY and RCSB PDB within the terms of the pre-defined criteria (Table 3):

- one worldwide approved typical antipsychotic: Chlorpromazine (CHL);
- two worldwide approved atypical antipsychotics: Risperidone (RIS) and Haloperidol (HAL);
- one atypical antipsychotic approved only in Japan: Nemonapride, also known as Emonapride (EMO);
- one compound used in pharmacological research: Eticlopride (ETI).

From Table 3 it can be observed that EMO and ETI target only the DA receptors and no primary targets were classified

for them by The IUPHAR/BPS Guide to PHARMACOLOGY, Release Version 2021.4 since they are not worldwide approved antipsychotics. However, EMO was reported as an antagonist compound, with a high affinity for the 5-HT_{1A} receptor, respectively a lower affinity for two 5-HT₂ receptors (5-HT_{2A} and 5-HT_{2C}) (Andersen et al., 1996; Clarke, 2007). Meanwhile ETI, as a control compound, has been described as an inhibitor of 5-HT₁ and 5-HT₂ receptors in the case of male Sprague-Dawley rats (Hall et al., 1985, 1986).

By reduction of MW of five scaffold donors resulted in a set of three scaffolds for each donor with one, respectively two substitution points (Figure 2). MarvinSketch was used for drawing, displaying, 2D optimization, and graphical processing of 2D images made for all scaffolds, MarvinSketch version 19.9.0, ChemAxon (<https://chemaxon.com/>).

3.1.2. Generation of the combinatorial library

By combining the 15 scaffolds (Figure 2) with the seven BBs (Figure 1) via a pseudo linker, SmiLib v2.0 rc2 generated a combinatorial library with 315 virtual derivatives. The generated combinatorial library consists in five sub-sets of virtual derivatives, corresponding to the five scaffold donors and each sub-set includes 63 virtual derivatives.

3.2. VS of combinatorial library

VS performed with FAF-Drugs4 on the five scaffold donors (the antipsychotics were used as a control compounds) revealed that all the five antipsychotics have a good bioavailability according with Egan's rule (Egan et al., 2000) and Veber's rule (Veber et al., 2002) and are drug-like compounds according with RO5; only CHL had one violation of RO5 (Table 4). Moreover, all the five antipsychotics were classified as free of covalent inhibitors and PAINS and fully compliant

with Fsp3, GSK 4/400 and MedChem rules, but some of them present a series of toxicological concerns (Table 5).

From Table 4 it can be observed that only CHL, a worldwide approved antipsychotic from the first generation, had one violation of RO5 (in terms of higher value for LogP), but fits within general RO5 specifications because one violation of RO5 is a good outcome (Lipinski, 2016; Lipinski et al., 2001, 2012). Therefore, all scaffold donors comply with the basic rules governing the ADME profile of good drug candidates (Table 2), as expected. Even though that RIS has an HBA outside of the threshold set for activity at the CNS level, this atypical antipsychotic is active at the CNS level, being able to penetrate BBB (Arnt & Skarsfeldt, 1998; Burns, 2001).

From computed data presented in Table 5 it can be observed that only RIS can be considered a safe compound (toxicologically speaking), being the single control compound that is not an iPPi; protein-protein interactions (PPIs) being "druggable" targets for a broad range of therapeutic areas—including CNS disorders (Ganapathiraju et al., 2016; Thanontip et al., 2019). The UMSs identified in the structure of four of the five control compounds (CHL, RIS, HAL and EMO) are considered as low-risk substructures and, more important, the amount of those substructures, are (even cumulated in the case of HAL) below the rejection thresholds. CHL and HAL were identified as Phl, which indicates a higher occurrence of possible side effects due to the intracellular accumulation of phospholipids in cells exposed to the cationic amphiphilic compounds. The fraction of sp³ hybridized carbons, evaluated within the framework of the Fsp3 rule, makes the compound have a more elaborated 3D shape; meanwhile, the increased number of the chiral centres increases the number of potential isomers of the compound. Such effects on molecular shape might allow for improved interactions with the target protein, enhancing the potency and/or specificity of the drug prototypes and

Table 8. P-LD results: BA of best drug candidates against selected targets (5-HT and DA receptors).

P-LD runs against 5-HT receptors					
DC for 5-HT _{1B} 4IAR (Wang et al., 2013)	BA (kcal/mol)	DC for 5-HT _{1D} 7E32 (Xu et al., 2021)	BA (kcal/mol)	DC for 5-HT _{2A} 6A93 (Kimura et al., 2019)	BA (kcal/mol)
ERM	-11.9	HAL_1.1_3_3_3	-10.5	HAL_1.1_3_3_3	-11.8
RIS	-10.9	HAL	-9.2	RIS	-11.4
HAL_1.1_3_3_3	-10.9	ETI_3.1_1_57_57	-8.9	HAL	-9.5
ETI_3.1_3_59_59	-10.1	RIS	-8.9	ETI_3.1_3_59_59	-9.2
ETI_3.1_1_57_57	-9.7	EMO	-8	ETI_3.1_1_57_57	-9.9
HAL	-9.3	ETI_3.1_3_59_59	-8	ETI	-7.4
EMO	-8.7	ETI	-7.6	EMO	-9.4
ETI	-7.6	5-HT	-6.2	CHL	-8.4
CHL	-7.4	CHL	-5.9	NA	NA
P-LD runs against DA receptors					
DC for D ₂ 6CM4 (Wang et al., 2018)	BA (kcal/mol)	DC for D ₃ 3PBL (Chien et al., 2010)	BA (kcal/mol)	DC for D ₄ 5WIU (Wang et al., 2017)	BA (kcal/mol)
HAL_1.1_3_3_3	-11.4	HAL_1.1_3_3_3	-11.6	RIS	-11.7
RIS	-11.4	RIS	-10.7	ETI_3.1_1_57_57	-10.5
ETI_3.1_1_57_57	-9.7	HAL	-9.1	ETI_3.1_3_59_59	-10.3
HAL	-9.5	EMO	-8.7	HAL_1.1_3_3_3	-9.9
EMO	-9.3	ETI_3.1_3_59_59	-8.4	EMO	-9.7
ETI_3.1_3_59_59	-8.9	ETI_3.1_1_57_57	-8.3	HAL	-9.5
ETI	-7.9	ETI	-7.9	CHL	-8.0
CHL	-7.1	CHL	-7.1	ETI	-7.8

DC: docking complexes; **BOLDED TARGET RCSB PDB ID:** the identifier of 3D structure used for the corresponding P-LD run [reference for the 3D structure of target used in the P-LD run]; ERM: Ergotamine (an alpha-1 selective adrenergic agonist vasoconstrictor used in the treatment of migraine disorders – ERM is the co-crystallized ligand from the experimental 3D structure of 5-HT_{1B}); **UNDERLINED LIGAND ID:** re-docking of the co-crystallized ligand from the experimental 3D structure of the target (reference ligand); NA: not assigned because in this particular P-LD run the reference ligand was one of the scaffold donors – RIS.

increasing the probability that it will lead to a successful drug. Such molecular shape effects could enable enhanced interactions with target proteins, improve the potency and/or specificity of drug prototypes, and increase the likelihood of obtaining a good drug. Therefore, ETI—the compound used in pharmacological research—has the highest score and probability that it will lead to the development of a successful drug. Predictions referring at Ro3.75 indicate that all of the control compounds are far from ideal models: $\text{LogP} > 3$ and $\text{tPSA} < 75 \text{ \AA}^2$ —those values being considered thresholds for a chemical profile with less adverse effects (check Table 4 for computed values). All scaffold donors fitted perfectly within the thresholds of GSK 4/400 and MedChem rules.

VS carried out with FAF-Drugs4 (Supplemental Table S1) identified only three virtual derivatives (VDs) as good drug candidates with predicted CNS activity (via passive BBB permeability—Table 6) and without high-risk UMSs and other major toxicity concerns (Table 7):

- one HAL derivative, namely HAL_1.1_3_3_3, with one inherited low-risk structural alert ("Low_Risk_halogenure_F") below the rejection threshold;
- two ETI derivatives: ETI_3.1_1_57_57 and ETI_3.1_3_59_59, both without any structural alerts.

From Table 6 it can be observed that all three investigated VDs have a maximum of two violations of RO5 (in terms of a higher value for MW for HAL_1.1_3_3_3, respectively a higher value for LogP for all three VDs), but all fit within general RO5 specifications because maximum two violations of RO5 represents an acceptable outcome (Lipinski, 2016; Lipinski et al., 2001, 2012). Therefore, all three investigated VDs comply with the rules governing the ADME profile of good drug candidates, with a predicted good bioavailability (including here both Veber's and Egan's rules for oral bioavailability). Moreover, all three VDs perfectly fit within the thresholds of the CNS filter, meaning that they can passively penetrate BBB.

Table 9. Comparative presentation of the simplified energy overview of P-LD run against 5-HT_{2A} (6A93) for novel hit and RIS (re-docking of the co-crystallized ligand) versus experimental data extracted from the PDB file available for 5-HT_{2A} (6A93).

RIS: Experimental data extracted from PDB file available for 5-HT_{2A} (6A93) (re-ranking scoring protocol applied to the experimental data)

Descriptor	Value	MolDock Score	Re-rank Weight	Re-rank Score
[I] External Ligand interactions		-150.84 (-150.805)		-131.947 (-131.919)
Protein – Ligand interactions		-150.84 (-150.805)		-131.947 (-131.919)
Steric (by PLP)	-150.686 (-150.686)	-150.686 (-150.686)	0.686 (0.686)	-103.37 (-103.37)
Steric (by LJ12-6)	-53.386 (-53.386)		0.533 (0.533)	-28.455 (-28.455)
Hydrogen bonds	-0.154 (-0.119)	-0.154 (-0.119)	0.792 (0.792)	-0.122 (-0.094)
[II] Internal Ligand interactions		11.34 (11.34)		13.675 (13.675)
Torsional strain	6.345 (6.345)	6.345 (6.345)	0.938 (0.938)	5.952 (5.952)
Torsional strain (sp2-sp2)	0 (0)		0.636 (0.636)	0 (0)
Hydrogen bonds	0 (0)			0 (0)
Steric (by PLP)	4.995 (4.995)	4.995 (4.995)	0.172 (0.172)	0.859 (0.859)
Steric (by LJ12-6)	49.379 (49.379)		0.139 (0.139)	6.864 (6.864)
[III] Total Energy ([I] + [II] = [III])		-139.5 (-139.464)		-118.272 (-118.244)
RIS: computed data for P-LD run against 5-HT_{2A} (6A93)				
Descriptors	Value	MolDock Score	Re-rank Weight	Re-rank Score
[I] External Ligand interactions		-154.57		-135.08
Protein – Ligand interactions		-154.57		-135.08
Steric (by PLP)	-154.57	-154.57	0.686	-106.035
Steric (by LJ12-6)	-54.493		0.533	-29.045
Hydrogen bonds	0	0	0.792	0
[II] Internal Ligand interactions		17.355		16.985
Torsional strain	5.167	5.167	0.938	4.846
Torsional strain (sp2-sp2)	0		0.636	0
Hydrogen bonds	0			0
Steric (by PLP)	12.188	12.188	0.172	2.096
Steric (by LJ12-6)	72.25		0.139	10.043
[III] Total Energy ([I] + [II] = [III])		-137.215		-118.094
HAL_1.1_3_3_3: computed data for P-LD run against 5-HT_{2A} (6A93)				
Descriptors	Value	MolDock Score	Re-rank Weight	Re-rank Score
[I] External Ligand interactions		-189.359		-164.809
Protein – Ligand interactions		-189.359		-164.809
Steric (by PLP)	-184.359	-184.359	0.686	-126.47
Steric (by LJ12-6)	-64.501		0.533	-34.379
Hydrogen bonds	-5	-5	0.792	-3.96
[II] Internal Ligand interactions		30.946		34.85
Torsional strain	18.844	18.844	0.938	17.676
Torsional strain (sp2-sp2)	4.189		0.636	2.664
Hydrogen bonds	0			0
Steric (by PLP)	12.102	12.102	0.172	2.081
Steric (by LJ12-6)	89.41		0.139	12.428
[III] Total Energy ([I] + [II] = [III])		-154.413		-129.96

Empty cells: data not applicable or not computed for respective descriptor; Value: the various terms on which the MolDock Score and the Re-rank Score are based on the MolDock Score: this column shows how the MolDock score energy is composed (the sum of a subset of the Value terms in which all terms are given the same weight); Re-rank Weight: summations of coefficients for the weighted Rerank Score; Rerank Score: scoring function which uses a weighted combination of the terms used by the MolDock score mixed with additional terms: the Steric (by PLP) term which use a PLP to approximate the steric energy, respectively the Steric (by LJ12-6) term which is the LJ12-6 approximation of the steric energy.

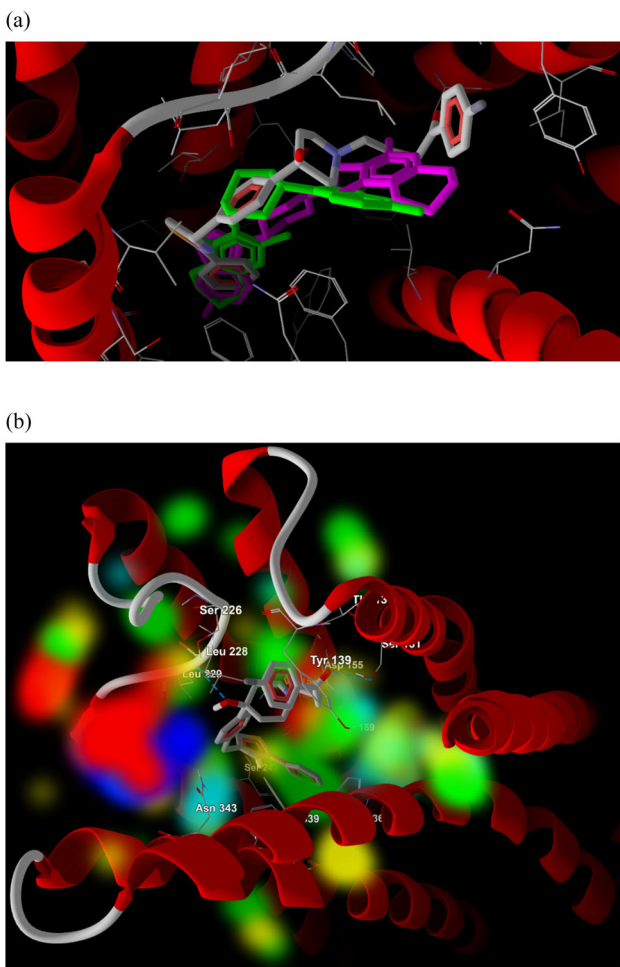


Figure 3. 3D depiction of the P-LD run against 5-HT_{2A} (6A93 – target is presented as a wireframe with secondary structure drawn as a cartoon, meanwhile ligands are figured as sticks) with (a) superimposing of the experimental structure of RIS extracted from PDB file available for 5-HT_{2A} (coloured in fuchsia), the best re-docking pose of RIS (coloured in green) and best docking pose of HAL_1.1_3_3_3 (coloured with the standard CPK colours); (b) graphical depiction of the binding mode of the best pose of HAL_1.1_3_3_3 (coloured with the standard CPK colours), the two H-bonds (depicted as thin interrupted blue lines) established with Ser131 and Leu229 residues of 5-HT_{2A}) and visualization of energy potential fields of the target protein (steric favourable regions are coloured in green, hydrogen acceptor favourable regions are coloured in turquoise, hydrogen donor favourable regions are coloured in yellow), the electrostatic potential of the target (generated using the MolDock [GRID] Score function (Thomsen & Christensen, 2006)) is depicted as follows: the red regions correspond to a nearby negative electrostatic charge, respectively the blue regions correspond to a nearby positive charge.

From Table 7 it can be observed that all three VDs are not iPPi, even though their scaffold donors (HAL and ETI) were detected as inhibitors of protein-protein interactions (see Table 5). Only in the structure of HAL_1.1_3_3_3 was detected an inherited low-risk substructure from its scaffold donor (HAL)—one Fluorine atom; value way below the rejection threshold (seven Fluorine atoms). Structures of ETI_3.1_1_57_57 and ETI_3.1_3_59_59 were found free of UMSs. As scaffold donors, three reported VDs are not covalent inhibitors. Besides, all three VDs were classified as non-inducers of phospholipidosis—in the context that its scaffold donor (HAL) was detected as Phl and is a worldwide approved atypical antipsychotic. Therefore, in the case of the investigated VDs, the occurrence of possible side effects caused by intracellular accumulation of phospholipids is unlikely to

appear, as predicted. In accordance with the Fsp3 rule, all three VDs scored slightly lower than their scaffold donors, but they present a sufficiently elaborated 3D shape to have good interactions with their molecular targets (DA and 5-HT receptors), indicating that those VDs are suitable candidates for P-LD and MD simulations. Predictions referring to Ro3.75 indicate that HAL_1.1_3_3_3 is a safer compound than its scaffold donor; meanwhile, no improvements were detected for the two VDs of ETI by comparison. However, 50% of the nuclear receptors compounds and 45% of allosteric modulators (approved drugs) fit in the problematic region of Ro3.75, while 30% of the bioavailable marketed drugs and 26% of iPPis populate this region (Lagorce et al., 2017). In concordance with GSK 4/400 rule, is predicted an unfavourable ADME-Tox profile for all three VDs, despite the fact that the two scaffold donors (HAL and ETI) had scored perfectly within the limits imposed by this rule—in defiance of the well-known toxicity issues of HAL, as an approved anti-psychotic drug, from Real World Data (RWD), Real World Evidence (RWE) and scientific literature (Aga et al., 2020; Barnes & Edwards, 1993; Cobaugh et al., 2007; Edwards & Barnes, 1993; Kondej et al., 2018). All three VDs comply with all conditions imposed by the regular settings implemented for MedChem rules in FAF-Drugs4.

3.3. VS of best drug-like candidates

3.3.1. P-LD runs for three selected VDs as best drug candidates

The results of the five docking simulations are presented briefly in Table 8, showing the binding affinity (BA) of the best docking poses for each docking run; as scoring criteria for the selection of the best pose of each ligand were used the zero values of the two root-mean-square deviation variants (RMSD lower bound and RMSD upper bound).

From Table 8 it can be observed that HAL_1.1_3_3_3 has the highest binding activity from all screened compounds (including here the co-crystallized ligands and all scaffold donors) against the 5-HT_{2A}, 5-HT_{1D}, D₂ and D₃ receptors. We are emphasizing the fact that its scaffold donor (HAL) has as primary targets three of those four receptors (5-HT_{2A}, D₂ and D₃ receptors) in accordance with The IUPHAR/BPS Guide to PHARMACOLOGY, Release Version 2021.4. Moreover, HAL_1.1_3_3_3 was found to have also a high BA against 5-HT_{1B} receptor (-10.9 kcal/mol), but slightly below BA of ERM (the co-crystallized ligand from the experimental 3D structure of this target—4IAR (Wang et al., 2013)) and RIS; however, no data was recorded in the last update of the aforementioned database about possible interactions of HAL with this target (NC-IUPHAR, 2022). HAL_1.1_3_3_3 exhibited a good BA (-9.9 kcal/mol) for the D4 receptor, but slightly lesser than the binding affinities of the other two VDs (ETI_3.1_1_57_57 and ETI_3.1_3_59_59), it is noted that this receptor is a primary target in humans of HAL in accordance with The IUPHAR/BPS Guide to PHARMACOLOGY, Release Version 2021.4 (Harding et al., 2022; Lahti et al., 1993; Shahid et al., 2009; Tice et al., 1994). Additionally, the BA of HAL_1.1_3_3_3 for D4 receptor is slightly better than BA of EMO (the co-

crystallized ligand from the experimental 3D structure of 5WIU (Wang et al., 2017) and other three antipsychotic compounds used as scaffold donors (HAL, CHL and ETI). Docking results show that from the two VDs of ETI, only ETI_3.1_3_59_59 is a good binder for only two targets: 5-HT_{1B} receptor ($BA = -10.1$ kcal/mol), respectively D₄ receptor ($BA = -10.3$ kcal/mol). Meanwhile, ETI_3.1_1_57_57 has a good binding affinity only for D₄ receptor ($BA = -10.5$ kcal/mol).

Summarizing the data presented in Table 8, it can be concluded that HAL_1.1_3_3_3 is a novel hit—"magic shotgun" type (Roth et al., 2004); able to strongly bind with five of the

investigated targets (best binder for 5-HT_{2A}, 5-HT_{1D}, D₂ and D₃ receptors; respectively strong binder for 5-HT_{1B} receptor).

The detailed information about energy interactions revealed by P-LD run against 5-HT_{2A} (6A93) after applying the re-ranking procedure for the best poses of docking complexes made by the novel hit (HAL_1.1_3_3_3) by comparing with RIS, the co-crystallized ligand of this target (from a double perspective: data extracted from the PDB file containing the co-crystallized ligand and its target—6A93 (Kimura et al., 2019) and re-docking of the co-crystallized ligand with the same molecular target) are showed in Table 9. The graphical

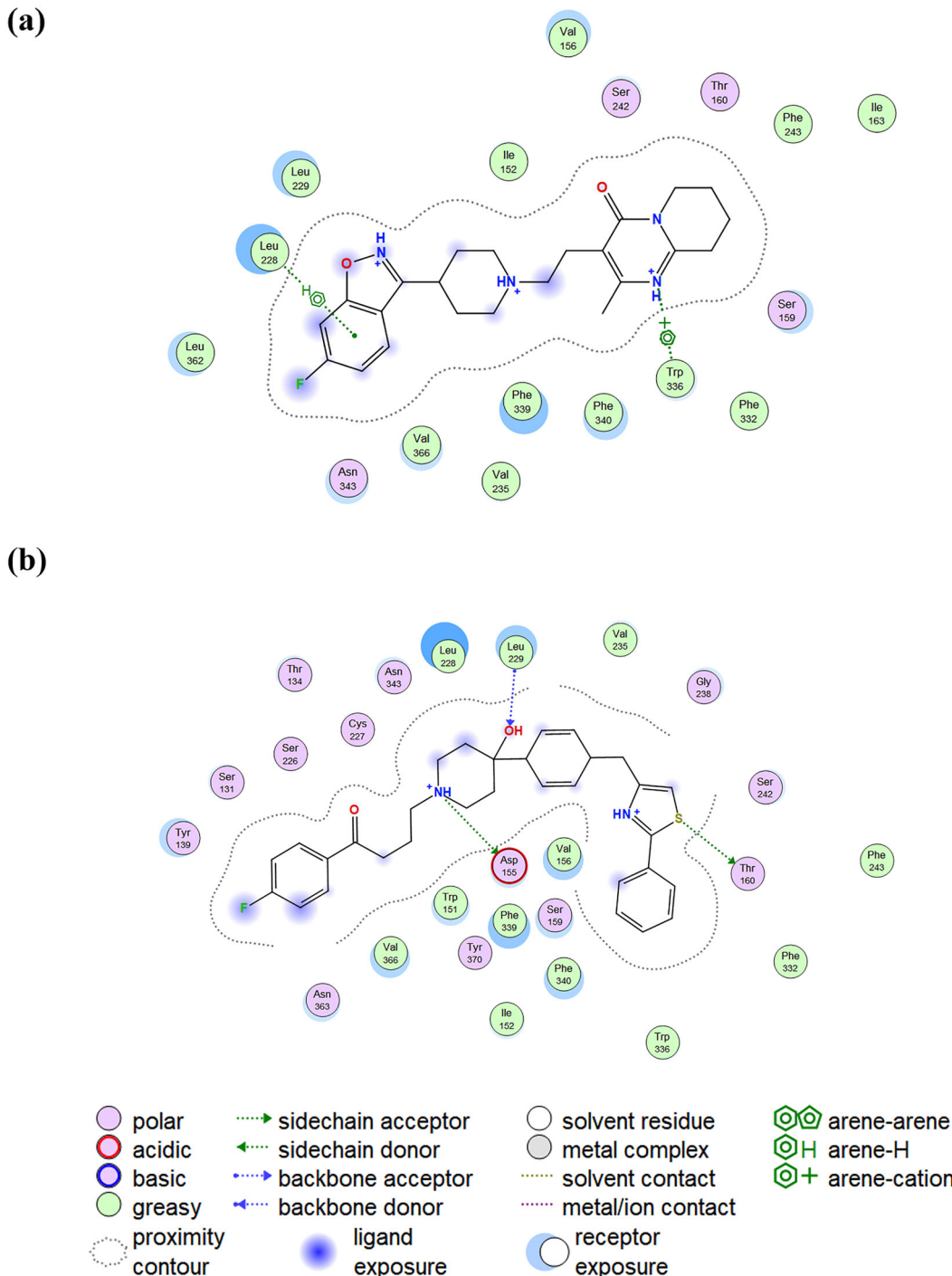


Figure 4. 2D protein-ligand interaction diagrams of the P-LD run against 5-HT_{2A} with (a) superimposing of the experimental structure of RIS extracted from the PDB file available for 5-HT_{2A}, best re-docking pose of RIS and best docking pose of HAL_1.1_3_3_3; (b) graphical depiction of the binding mode of the best pose of HAL_1.1_3_3_3; the three H-bond donor/acceptor interactions are predicted for HAL_1.1_3_3_3 established by Leu229, Asp155, and Thr160 residues.

depiction of the aforementioned protein—ligands interactions is illustrated in [Figure 3](#) (using functionalities of the Molegro Molecular Viewer 2.5) and [Figure 4](#).

By analyzing data presented in [Table 9](#) and the graphical depiction of protein—ligands interactions illustrated in [Figures 3a](#) and [4](#) it can be observed that the P-LD run against 5-HT_{2A} (6A93) is a valid simulation taking into account both the energy interactions and the spatial orientation of the re-docked control ligand (RIS) by comparison with the co-crystallized ligand (RIS) and its target from the experimental structure of 5-HT_{2A} (6A93). Analyzing the binding pattern of HAL_1.1_3_3_3 depicted in [Figures 3b](#) and [4](#) it can be noticed that this novel hit establishes two strong H-bonds with amino acids located in the second transmembrane helix (Ser131) and an extracellular topological domain (Leu229), meanwhile, RIS doesn't have such interactions (H-bonds) with the target. Furthermore, Leu229 is a binding site known as a hydrophobic barrier that decreases the speed of ligand binding and dissociation (Wacker et al., 2017). Therefore, this binding pattern explains the high BA of HAL_1.1_3_3_3 for the 5-HT_{2A} receptor.

3.3.2. MD simulations

To confirm our previous findings, the HAL_1.1_3_3_3 ligand was chosen for the MD simulations as a molecule exhibiting the highest affinities against 5-HT and DA receptors ([Figure 5](#)). This novel hit was found to be highly potent against the 5-HT_{2A} receptor with the lowest Gibbs free energy value (-11.8 kcal/mol). Therefore, we measured free energy between the hit molecule and the human 5-HT_{2A} receptor using HAL as a reference. The analysis was performed by obtaining the vdW and electrostatic interaction energies, where the ΔG_{lie} values were found to be -61.93 kcal/mol for the novel hit and only -55.48 kcal/mol for the reference ([Figure 6a](#)).

On the other hand, ΔG_{lie} and its ΔE_{vdW} component were detected to be mainly above the energy threshold ($E = -60$ kcal/mol) for the reference and below for the novel

hit ([Figure 6b,c](#)). Additionally, the ΔE_{elec} component was determined to be close to the energy threshold ($E = -100$ kcal/mol) for both ligands but slightly lower for the novel hit ([Figure 6b,c](#)).

Additionally, the free energy of binding based on implicit solvation models was estimated for the 5-HT_{2A} transporter complexed with the HAL and novel hit molecules. The MM-PBSA/GBSA calculations ([Table 10](#)) were implemented, using representative structures obtained from 200 ns MD trajectories by the Fast Amber Rescoring method. They confirmed the previous data by revealing much higher binding affinities for the hit/5-HT_{2A} complex than for HAL/5-HT_{2A} ([Table 6](#)). The entropy-enthalpy compensation analysis revealed the endothermic process ($\Delta H > 0$) of protein-ligand interaction with the increased disorder ($T\Delta S > 0$), in which spontaneity depends on the temperature. The reference thermodynamic parameters (ΔH_0 and $T\Delta S_0$) were obtained as the experimental data from the binding assay for serotonin with 5-HT_{2A} (Dalpiaz et al., 1995).

On the other hand, to explore the movements of the studied complexes, the root-mean-square deviation (RMSD) and fluctuation (RMSF) values together with the radius of gyration (Rg), concerning the initial conformation were plotted versus time ([Figure 7a–e](#)). The protein RMSD values were lower (RMSD = 7.24 Å) in the HAL/5-HT_{2A} complex than in hit/5-HT_{2A} (RMSD = 9.39 Å) indicating more deviation of the latter from the initial state ([Figure 7a](#)). The ligand RMSD remained mostly below the 2.0 Å threshold for both complexes ([Figure 7b](#)). The receptor RMSF values produced some picks associated with the high flexibility of the N- and C-terminal parts and extracellular and intracellular loops ([Figure 7c](#)). Additionally, the intracellular BRIL domain experienced a significant conformational change upon the novel hit binding ([Figure 7c](#)). The atomic fluctuations of the novel hit showed reduced RMSF values in comparison to the reference ([Figure 7d](#)). The Rg values were associated with slightly higher 5-HT_{2A} compactness upon the hit binding, converging gradually to the same levels for both complexes after 150 ns

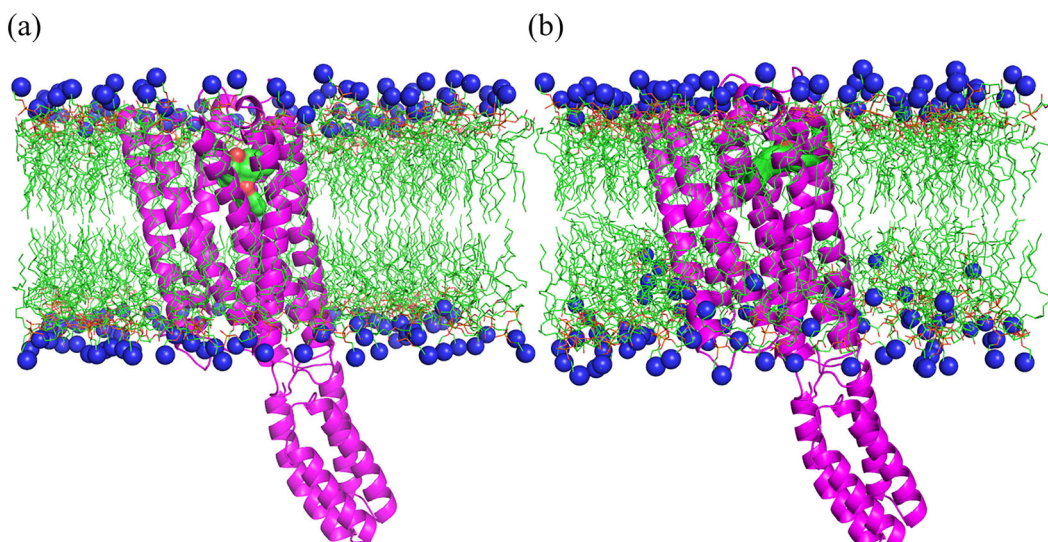


Figure 5. Protein-ligand systems embedded in lipid membrane bilayer including haloperidol (a) and novel hit (b). The ligand molecules are visualized using a molecular surface. All hydrogen molecules are omitted to enhance clarity.

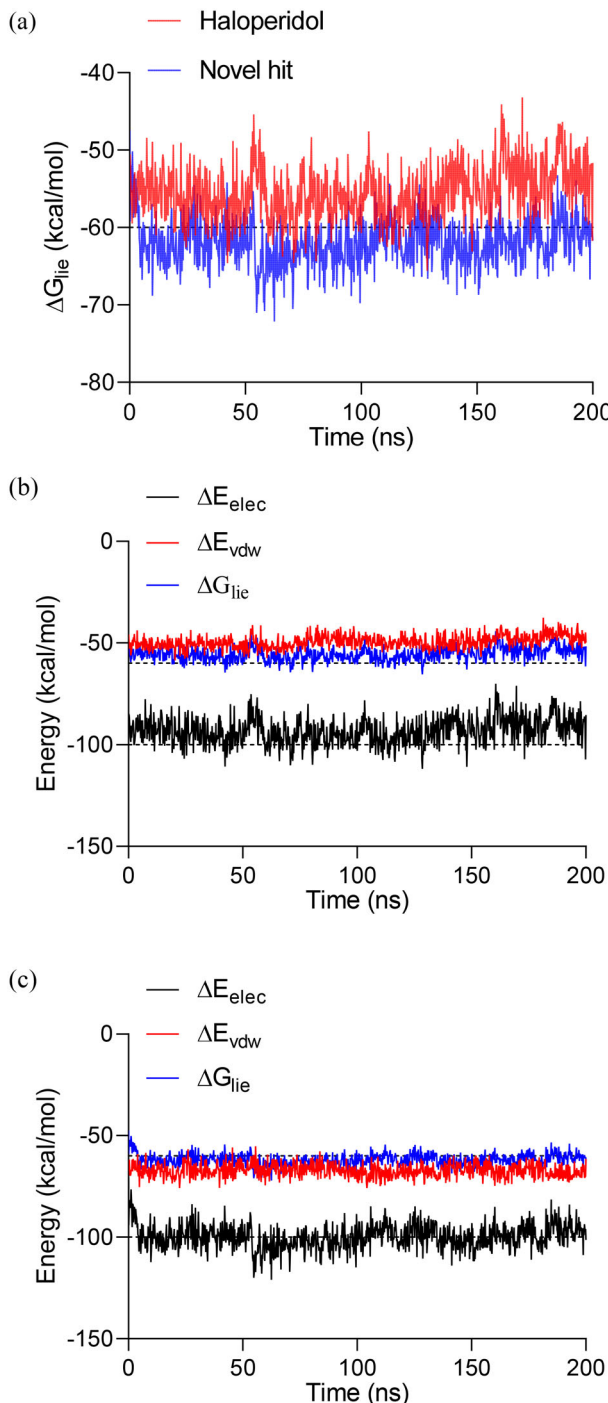


Figure 6. (a) Liner interaction energies (ΔG_{lie}) based on van der Walls (ΔE_{vdw}) and electrostatic (ΔE_{elec}) interactions measured for the (b) reference molecule (HAL) and (c) novel hit (HAL_1.1_3_3_3) during the 200 ns MD simulation as 5-HT_{2A} antagonists. The energy thresholds are shown as dashed lines.

Table 10. Summary of calculated energetic terms (kcal/mol and kcal*K/mol) for Hal and novel hit bound to 5-HT_{2A} receptor using MM-PBSA/GBSA methods.

Energy	HAL/5-HT _{2A}	hit/5-HT _{2A}
$\Delta G_{\text{PB/GBSA}}$	-17.86	-31.46
ΔH	44.69	78.74
$T\Delta S$	0.21	0.37
$\Delta \Delta H$	21.28	55.33
$T\Delta \Delta S$	0.09	0.26

$\Delta \Delta H \equiv \Delta H - \Delta H_0$; $T\Delta \Delta S \equiv (T\Delta S) - (T\Delta S_0)$.

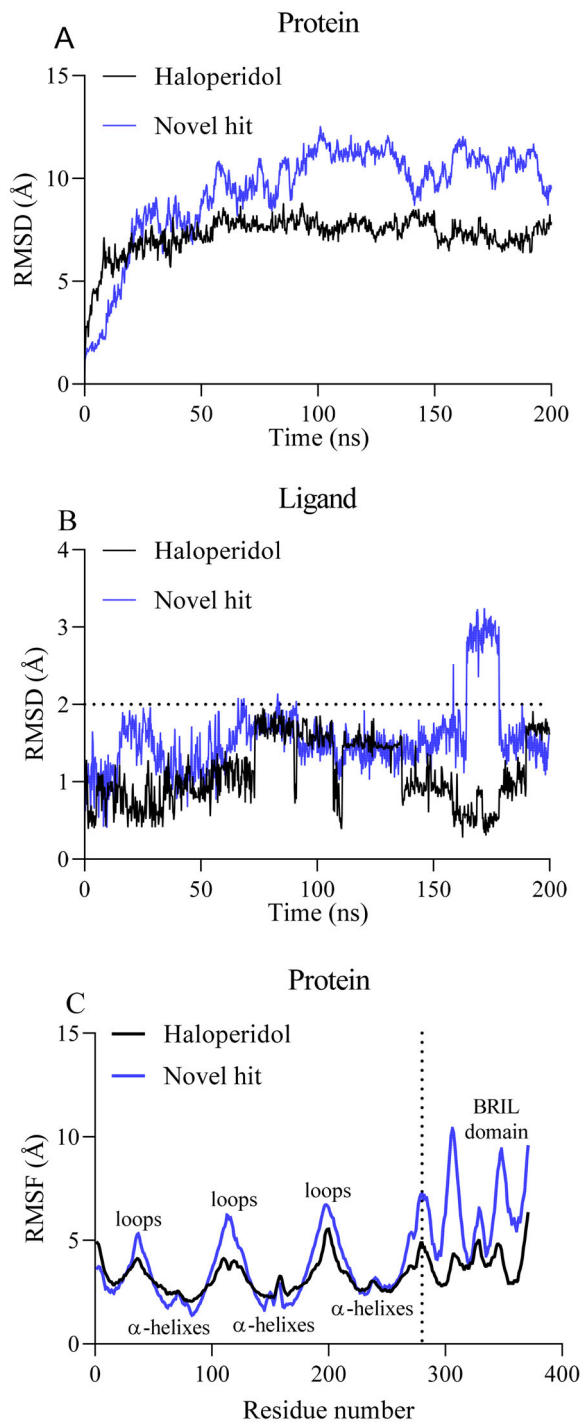


Figure 7. RMSD (a, b), RMSF (c, d), Rg (e), and contribution (%) of amino acid residues (f) involved in H-bonding calculated for HAL and novel hit bound to the 5-HT_{2A} receptor during 200 ns MD simulation. The threshold is depicted as a dotted line. The unique amino acids are marked with an asterisk.

(Figure 7e). Finally, the impact of receptor residues involved in the receptor-ligand interactions was assessed as a contribution (percentage) of each residue calculate from the total number of amino acids involved in H-binding (Figure 7f). The number of H-bond forming residues was the highest for hit/5-HT_{2A}, where most of them were detected for both complexes and some being unique only for HAL/5-HT_{2A} (Leu162) or HAL/5-HT_{2A} (Cys160, Trp253, and His3).

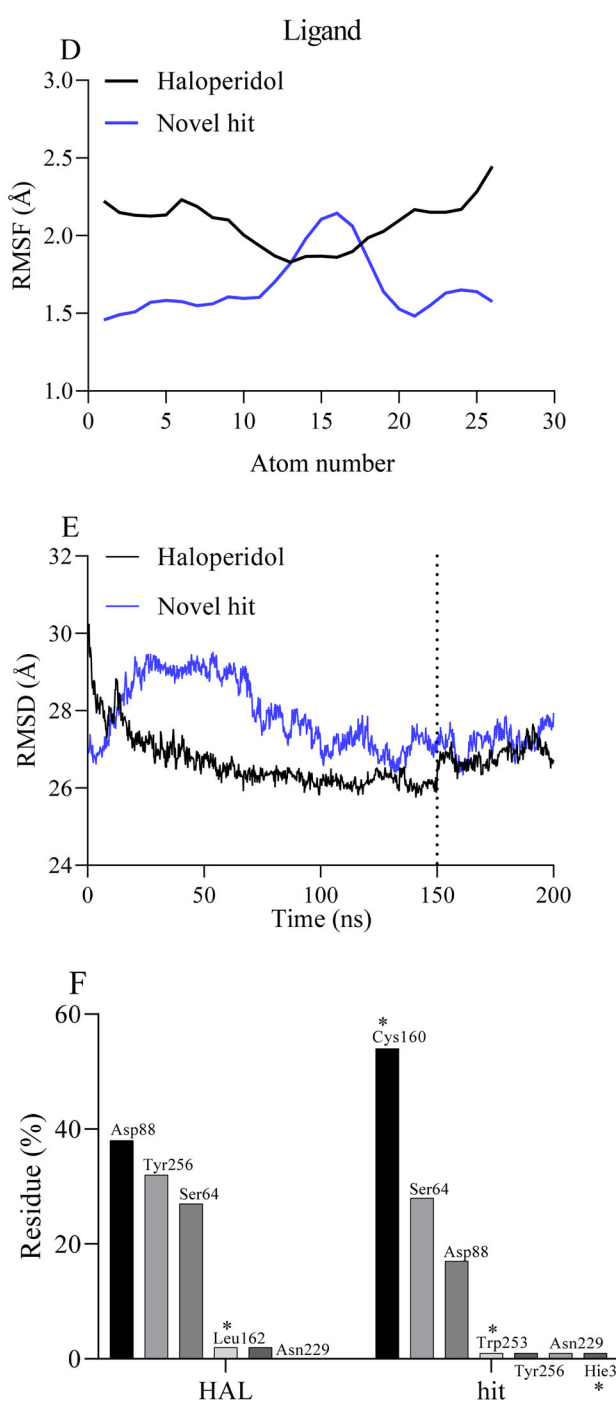


Figure 7. Continued

3.3.3. Permeation phenomena at the level of the BBB

The results of the individual assessment of the passive permeation phenomena at the BBB level of the best drug candidates and their scaffold donors (HAL and ETI) is presented hereafter in Table 11, whilst the predictions made for P-gp affinity (including here the active transmembrane transport at the BBB level) are presented in Table 11.

From Table 11 it can be observed that HAL_1.1_3_3_3 and its scaffold donor succeeded to comply with the threshold value set for the BBB permeability ($\log BB \geq 0.3$) (Kunwittaya et al., 2013) accordingly to the calculations done with one of the physicochemical-based descriptors ($\log BB_{Rishpon}$). At the

same time, the results of calculations made with the other physicochemical-based descriptor ($\log BB_{Clark}$) indicate that HAL_1.1_3_3_3 and its scaffold donor might comply with the $(BBB-) > \log BB > (BBB+)$ threshold (Shityakov et al., 2015; Shityakov & Förster, 2014). Furthermore, HAL_1.1_3_3_3 and its scaffold donor were positively evaluated for BBB permeability (BBB_{P-Prob}) and CNS permeability (LogPS) by advanced predictive models based on patterns—true “molecular/structural fingerprints”; predictors with high robustness, developed with the help of machine learning methods.

Data presented in Table 10 indicates the ETI and its VDs might be significantly less BBB permeable than HAL and its derivative. Moreover, the predictions made for the two VDs of ETI for BBB permeability (BBB_{P-Prob}) with the sSPR-based model (implemented in the admetSAR software) were determined as marginal. Meanwhile, the other advanced predictor (implemented in the pkCSM web-server) classified them outside the optimal interval for good CNS permeability (LogPS).

The $\log BB$ values for HAL and RES produced by our *in silico* algorithm support the experimental BBB penetration determined for these reference molecules. In particular, the experimental $\log BB$ parameter for HAL ($\log BB = 1.34$) indicated its very high BBB permeation ($\log BB > 0.3$); while the experimental BBB permeation for RES was very poor ($\log BB = -0.02$) (Muehlbacher et al., 2011; Platts et al., 2001). The discrepancy between the experimental and theoretical $\log BB$ values for HAL was due to the activation of some influx transporters, such as organic cation transporter 1, to deliver this drug to the brain (Sekhar et al., 2019).

Data presented in Table 12 indicates that HAL_1.1_3_3_3 and its scaffold donor both have a good P-gp affinity, being classified simultaneously as P-gp substrates and P-gp inhibitors—the two software tools (the admetSAR software and the pkCSM web-server) used for predictions being in total consensus. The same total consensus of the two software tools was achieved only in the case of the classification of ETI and its two VDs as P-gp substrates, respectively in the case of the classification of ETI as P-gp non-inhibitor. ETI_3.1_1_57_57 and ETI_3.1_3_59_59 were differently classified by the two software tools. Taking in account that the pkCSM web-server surpasses the admetSAR software for the two P-gp inhibitor models with a statistically significant performance (Pires et al., 2015), it can be considered that two VDs of ETI are P-gp inhibitors (identical classifications made by P-gp inhibitor I model and P-gp inhibitor II model implemented in the pkCSM web-server).

3.3.4. Individual toxicological profiling of safest drug candidates

Results of the individual toxicological profiling of HAL and HAL_1.1_3_3_3 are summarized in Table 13, meanwhile the individual toxicological profiling of ETI and its VDs is presented in Table 14.

From the beginning, in Table 13, it can be observed that HAL_1.1_3_3_3 has a way lower acute oral toxicity than its scaffold donor ($LD50_{oral} = 800 \text{ mg/kg}$ vs $LD50_{oral} = 71 \text{ mg/kg}$) and its predicted toxicity class (4) is safer than the toxicity class predicted for its scaffold donor (3). To be noted

Table 11. Passive BBB permeation for the best drug candidates and their scaffold donors.

Compound	LogBB _{Clark}	LogBB _{Rishton}	BBB _{P-Prob} [+](by admetSAR)	LogPS (by pkCSM)
HAL	0.17	0.41	0.9465	-0.104
HAL_1.1_3_3_3	-0.07	0.37	0.9189	-1.799
ETI	-0.47	-0.14	0.7256	-2.919
ETI_3.1_1_57_57	-0.42	0.07	0.5378	-2.169
ETI_3.1_3_59_59	-0.34	0.11	0.5378	-2.213

BBB_{P-Prob} [+]: indicates the positive outcome of BBB_{P-Prob} assessment; **Bold and italicized values:** values are outside of the threshold considered for activity at the CNS level via passive BBB permeability ($\log BB \geq 0.3$) (Kunwittaya et al., 2013); **bold and underlined values:** values are outside of the optimal interval for activity at the CNS level ($\log PS > -2$), but not in exclusion interval which includes compounds unable to have activity at the CNS level ($\log PS < -3$).

Table 12. Comparative computational evaluation of P-gp affinity probability for the best drug candidates and their scaffold donors.

Compound	P-gp substrate		P-gp inhibitor I		P-gp inhibitor II	
	By admetSAR (Prb)	By pkCSM (Cat)	By admetSAR (Prb)	By pkCSM (Cat)	By admetSAR (Prb)	By pkCSM (Cat)
HAL	Substrate (0.6673)	Substrate (YES)	Inhibitor (0.8563)	Inhibitor (YES)	Inhibitor (0.8137)	Inhibitor (YES)
HAL_1.1_3_3_3	Substrate (0.6122)	Substrate (YES)	Inhibitor (0.7204)	Inhibitor (YES)	Inhibitor (0.6827)	Inhibitor (YES)
ETI	Substrate (0.8398)	Substrate (YES)	Non-Inhibitor (0.8606)	Inhibitor (NO)	Non-Inhibitor (0.5545)	Inhibitor (NO)
ETI_3.1_1_57_57	Substrate (0.7803)	Substrate (YES)	Non-Inhibitor (0.8487)	Inhibitor (YES)	Non-Inhibitor (0.6072)	Inhibitor (YES)
ETI_3.1_3_59_59	Substrate (0.7803)	Substrate (YES)	Non-Inhibitor (0.8487)	Inhibitor (YES)	Non-Inhibitor (0.6072)	Inhibitor (YES)

admetSAR (Prb): probability of being P-gp substrate or P-gp inhibitor – implemented only in the admetSAR software; pkCSM (Cat): the pkCSM web-server use a “categorical” classification method: YES and NO.

Table 13. Predicted toxicity models for HAL and its VD.

Toxicity Model Report	HAL	HAL_1.1_3_3_3
LD50 _{oral} (mg/kg)	71	800
TC/Av-S (%)/P-Acc (%)	3/100/100	4/53.82/67.38
Hepatotoxicity ^{OT} /Prb	Inactive/0.96	Inactive/0.73
Carcinogenicity ^{TEP} /Prb	Inactive/0.54	Inactive/0.61
Immunotoxicity ^{TEP} /Prb	Inactive/0.64	Inactive/0.83
Mutagenicity ^{TEP} /Prb	Inactive/0.89	Inactive/0.80
Cytotoxicity ^{TEP} /Prb	Inactive/0.72	Inactive/0.69
AhR ^{Tox21-NRS} /Prb	Inactive/0.97	Inactive/0.84
AR ^{Tox21-NRS} /Prb	Inactive/0.99	Inactive/0.98
AR-LBD ^{Tox21-NRS} /Prb	Inactive/1.00	Inactive/0.98
Aromatase ^{Tox21-NRS} /Prb	Inactive/0.99	Inactive/0.85
ER ^{Tox21-NRS} /Prb	Inactive/0.97	Inactive/0.79
ER-LBD ^{Tox21-NRS} /Prb	Inactive/0.99	Inactive/0.93
PPAR-Gamma ^{Tox21-NRS} /Prb	Inactive/0.99	Inactive/0.90
nrf2/ARE ^{Tox21-SR} /Prb	Inactive/0.97	Inactive/0.92
HSE ^{Tox21-SR} /Prb	Inactive/0.97	Inactive/0.92
MMP ^{Tox21-SR} /Prb	Inactive/0.70	Inactive/0.62
p53 ^{Tox21-SR} /Prb	Inactive/0.99	Inactive/0.92
ATAD5 ^{Tox21-SR} /Prb	Inactive/0.99	Inactive/0.96

LD50_{oral}: predicted acute toxicity expressed as lethal dose for oral toxicity; TC: predicted toxicity class based on LD50_{oral}; Av-S: average similarity with compounds included in the database; P-Acc: prediction accuracy; ^{OT}: organ toxicity; Prb: probability; ^{TEP}: Toxicity endpoints; ^{Tox21-NRS}: Tox21-Nuclear receptor signalling pathways; ^{Tox21-SR}: Tox21-Stress response pathways; AhR: Aryl hydrocarbon Receptor; AR: Androgen Receptor; AR-LBD: Androgen Receptor Ligand Binding Domain; ER: Estrogen Receptor; ER-LBD: Estrogen Receptor Ligand Binding Domain; PPAR-Gamma: Peroxisome Proliferator-Activated Receptor Gamma; nrf2/ARE: Nuclear factor (erythroid-derived 2)-like 2/antioxidant responsive element; HSE: Heat shock factor response element; MMP: Mitochondrial Membrane Potential; p53: Phosphoprotein (Tumor Suppressor) p53; ATAD5: ATPase family AAA domain-containing protein 5.

that average similarity and prediction accuracy made for the toxicity class of HAL have maximum values ($TC = 100$ and $Av-S = 100\%$), which indicate that HAL and experimental data about HAL are included in the training set used by the developers of the ProTox-II web-server. Both tested compounds were classified as inactive for hepatotoxicity, all of

Table 14. Predicted toxicity models for ETI and its two VDs.

Toxicity Model Report	ETI	ETI_3.1_1_57_57	ETI_3.1_3_59_59
LD50 _{oral} (mg/kg)	576	1000	1000
TC/Av-S (%)/P-Acc (%)	4/77.54/69.26	4/49.9/54.26	4/46.32/54.26
Hepatotoxicity ^{OT} /Prb	Inactive/0.81	Inactive/0.65	Inactive/0.65
Carcinogenicity ^{TEP} /Prb	Inactive/0.65	Inactive/0.64	Inactive/0.64
Immunotoxicity ^{TEP} /Prb	Active/0.54	Inactive/0.89	Inactive/0.94
Mutagenicity ^{TEP} /Prb	Inactive/0.71	Inactive/0.68	Inactive/0.68
Cytotoxicity ^{TEP} /Prb	Inactive/0.65	Inactive/0.59	Inactive/0.59
AhR ^{Tox21-NRS} /Prb	Inactive/0.99	Inactive/0.90	Inactive/0.90
AR ^{Tox21-NRS} /Prb	Inactive/1.00	Inactive/0.97	Inactive/0.97
AR-LBD ^{Tox21-NRS} /Prb	Inactive/1.00	Inactive/0.93	Inactive/0.93
Aromatase ^{Tox21-NRS} /Prb	Inactive/0.99	Inactive/0.86	Inactive/0.86
ER ^{Tox21-NRS} /Prb	Inactive/0.96	Inactive/0.90	Inactive/0.90
ER-LBD ^{Tox21-NRS} /Prb	Inactive/0.99	Inactive/0.95	Inactive/0.95
PPAR-Gamma ^{Tox21-NRS} /Prb	Inactive/0.99	Inactive/0.88	Inactive/0.88
nrf2/ARE ^{Tox21-SR} /Prb	Inactive/0.99	Inactive/0.93	Inactive/0.93
HSE ^{Tox21-SR} /Prb	Inactive/0.99	Inactive/0.93	Inactive/0.93
MMP ^{Tox21-SR} /Prb	Inactive/0.98	Inactive/0.79	Inactive/0.79
p53 ^{Tox21-SR} /Prb	Inactive/0.99	Inactive/0.83	Inactive/0.83
ATAD5 ^{Tox21-SR} /Prb	Inactive/0.99	Inactive/0.97	Inactive/0.97

LD50_{oral}: predicted acute toxicity expressed as lethal dose for oral toxicity; TC: predicted toxicity class based on LD50_{oral}; Av-S: average similarity with compounds included in the database; P-Acc: prediction accuracy; ^{OT}: organ toxicity; Prb: probability; ^{TEP}: Toxicity endpoints; ^{Tox21-NRS}: Tox21-Nuclear receptor signalling pathways; ^{Tox21-SR}: Tox21-Stress response pathways; AhR: Aryl hydrocarbon Receptor; AR: Androgen Receptor; AR-LBD: Androgen Receptor Ligand Binding Domain; ER: Estrogen Receptor; ER-LBD: Estrogen Receptor Ligand Binding Domain; PPAR-Gamma: Peroxisome Proliferator-Activated Receptor Gamma; nrf2/ARE: Nuclear factor (erythroid-derived 2)-like 2/antioxidant responsive element; HSE: Heat shock factor response element; MMP: Mitochondrial Membrane Potential; p53: Phosphoprotein (Tumor Suppressor) p53; ATAD5: ATPase family AAA domain-containing protein 5.

the investigated toxicity endpoints, and Tox21 (all of the nuclear receptor signalling pathways and all of the stress response pathways).

By analyzing the data contained by Table 14, it can be stated that the two VDs of ETI exhibit lower acute oral toxicity than their scaffold donor (even lower than HAL_1.1_3_

3_3—see Table 12), but are categorized in the same toxicity class as ETI (4). Both VDs of ETI were classified as inactive for hepatotoxicity, all of the investigated toxicity endpoints, and Tox21, meanwhile ETI appears to be suspicious of causing immunotoxicity problems.

4. Conclusions

In this work, we designed and implemented the *in silico* pipeline to computationally synthesize novel compounds as leads using the standard drug scaffolds with improved PK/PD properties from the standard scaffolds. As an outcome, the HAL derivative (HAL_1.1_3_3_3) as a novel hit was identified with better affinity to the 5-HT_{2A}, 5-HT_{1D}, D₂, D₃, and 5-HT_{1B} receptors than the reference molecule. Moreover, this hit substance was predicted to maintain similar BBB permeation properties and much lower toxicological profiles in comparison to HAL. The proposed rational drug design platform might be an indispensable tool to develop novel antipsychotic drugs for the treatment of psychosis as a manifestation of schizophrenia, bipolar disorder, and severe depression.

Disclosure statement

No potential conflict of interest was reported by the author(s).

Institutional review board statement

"Not applicable"—*in silico* studies do not involve humans or animals and are compliant with the "Three Rs" in the European Union legislative framework.

Funding

We thank the supporting organization providing grant 075-15-2021-1349 and the ITMO Fellowship.

Author contributions

Conceptualization, R.T. and S.S.; methodology, R.T. and S.S.; software, R.T., Y.P.; validation, R.T. and S.S.; formal analysis, R.T.; investigation, R.T.; resources, R.T.; data curation, S.S.; writing—original draft preparation, R.T.; writing—review and editing, R.T., S.S.; visualization, R.T., S.S.; supervision, R.T., S.S.; project administration, R.T.; funding acquisition, S.S. "All authors have read and agreed to the published version of the manuscript."

Data availability statement

MD simulation data are kept by S.S. and available from S.S.; R.T is responsible for keeping and giving access to the data for the rest of the *in silico* work.

References

- Adenot, M., & Lahana, R. (2004). Blood-brain barrier permeation models: Discriminating between potential CNS and Non-CNS drugs including P-glycoprotein substrates. *Journal of Chemical Information and Computer Sciences*, 44(1), 239–248. <https://doi.org/10.1021/ci034205d>
- Aga, V. M., Shad, M. U., Zhu, H., & Salzman, C. (2020). Psychopharmacologic treatment. *Handbook of mental health and aging* (pp. 315–399). Elsevier. ISBN 9780128001363.
- Andersen, K., Liljefors, T., Hyttel, J., & Perregaard, J. (1996). Serotonin 5-HT₂ receptor, dopamine D₂ receptor, and α1 adrenoceptor antagonists. Conformationally flexible analogues of the atypical antipsychotic sertindole. *Journal of Medicinal Chemistry*, 39(19), 3723–3738. <https://doi.org/10.1021/jm960159f>
- Arnt, J., & Skarsfeldt, T. (1998). Do novel antipsychotics have similar pharmacological characteristics? A review of the evidence. *Neuropsychopharmacology: Official Publication of the American College of Neuropsychopharmacology*, 18(2), 63–101. [https://doi.org/10.1016/S0893-133X\(97\)00112-7](https://doi.org/10.1016/S0893-133X(97)00112-7)
- Baell, J. B., & Holloway, G. A. (2010). New substructure filters for removal of pan assay interference compounds (PAINS) from screening libraries and for their exclusion in bioassays. *Journal of Medicinal Chemistry*, 53(7), 2719–2740. <https://doi.org/10.1021/jm901137j>
- Bai, Y., Chen, G., Yang, H., & Gao, K. (2020). Do Asian and North American patients with bipolar disorder have similar efficacy, tolerability, and safety profile during clinical trials with atypical antipsychotics? *Journal of Affective Disorders*, 261, 259–270. <https://doi.org/10.1016/j.jad.2019.10.012>
- Banerjee, P., Eckert, A. O., Schrey, A. K., & Preissner, R. (2018). ProTox-II: A webserver for the prediction of toxicity of chemicals. *Nucleic Acids Research*, 46(W1), W257–W263. <https://doi.org/10.1093/nar/gky318>
- Barnes, T. R. E., & Edwards, J. G. (1993). The side-effects of antipsychotic drugs. I. CNS and neuromuscular effects. *Antipsychotic drugs and their side-effects* (pp. 213–247). Academic Press.
- Benigni, R., & Bossa, C. (2011). Mechanisms of chemical carcinogenicity and mutagenicity: A review with implications for predictive toxicology. *Chemical Reviews*, 111(4), 2507–2536. <https://doi.org/10.1021/cr100222q>
- Berman, H. M. (2003). The protein data bank. *Leadership in science and technology: A reference handbook* (Vol 44, pp. 661–667). SAGE Publications, Inc.
- Berman, H. M., Westbrook, J., Feng, Z., Gilliland, G., Bhat, T. N., Weissig, H., Shindyalov, I.N., & Bourne, P. E. (2000). The protein data bank. *Nucleic Acids Research*, 28(1), 235–242. <https://doi.org/10.1093/nar/28.1.235>
- Blagg, J. (2010). Structural alerts for toxicity. In D. J. Abraham (Ed.), *Burger's medicinal chemistry and drug discovery* (pp. 301–334). John Wiley & Sons, Inc. ISBN 0471266949.
- Broccatelli, F., Carosati, E., Neri, A., Frosini, M., Goracci, L., Oprea, T. I., & Cruciani, G. (2011). A novel approach for predicting P-glycoprotein (ABCB1) inhibition using molecular interaction fields. *Journal of Medicinal Chemistry*, 54(6), 1740–1751. <https://doi.org/10.1021/jm101421d>
- Bruns, R. F., & Watson, I. A. (2012). Rules for identifying potentially reactive or promiscuous compounds. *Journal of Medicinal Chemistry*, 55(22), 9763–9772. <https://doi.org/10.1021/jm301008n>
- Burley, S. K., Bhikadiya, C., Bi, C., Bittrich, S., Chen, L., Crichlow, G. V., Christie, C. H., Dalenberg, K., Di Costanzo, L., Duarte, J. M., Dutta, S., Feng, Z., Ganesan, S., Goodsell, D. S., Ghosh, S., Green, R. K., Guranović, V., Guzenko, D., Hudson, B. P., ... Zhuravleva, M. (2021). RCSB Protein Data Bank: Powerful new tools for exploring 3D structures of biological macromolecules for basic and applied research and education in fundamental biology, biomedicine, biotechnology, bioengineering and energy sciences. *Nucleic Acids Research*, 49(D1), D437–D451. <https://doi.org/10.1093/nar/gkaa1038>
- Burley, S. K., Bhikadiya, C., Bi, C., Bittrich, S., Chen, L., Crichlow, G. V., Duarte, J. M., Dutta, S., Fayazi, M., Feng, Z., Flatt, J. W., Ganesan, S. J., Goodsell, D. S., Ghosh, S., Kramer Green, R., Guranovic, V., Henry, J., Hudson, B. P., Lawson, C. L., ... Zardecki, C. (2022). RCSB Protein Data Bank: Celebrating 50 years of the PDB with new tools for understanding and visualizing biological macromolecules in 3D. *Protein Science: A Publication of the Protein Society*, 31(1), 187–208. <https://doi.org/10.1002/pro.4213>
- Burns, M. J. (2001). The pharmacology and toxicology of atypical anti-psychotic agents. *Journal of Toxicology. Clinical Toxicology*, 39(1), 1–14. <https://doi.org/10.1081/CLT-100102873>

- Cantù, F., Ciappolino, V., Enrico, P., Moltrasio, C., Delvecchio, G., & Brambilla, P. (2021). Augmentation with atypical antipsychotics for treatment-resistant depression. *Journal of Affective Disorders*, 280(Pt A), 45–53. <https://doi.org/10.1016/j.jad.2020.11.006>
- Chen, L., Li, Y., Zhao, Q., Peng, H., & Hou, T. (2011). ADME evaluation in drug discovery. 10. Predictions of P-glycoprotein inhibitors using recursive partitioning and Naive Bayesian classification techniques. *Molecular Pharmaceutics*, 8(3), 889–900. <https://doi.org/10.1021/mp100465q>
- Cheng, F., Li, W., Zhou, Y., Shen, J., Wu, Z., Liu, G., Lee, P. W., & Tang, Y. (2012). admetSAR: A comprehensive source and free tool for assessment of chemical ADMET properties. *Journal of Chemical Information and Modeling*, 52(11), 3099–3105. <https://doi.org/10.1021/ci300367a>
- Cheng, T., Zhao, Y., Li, X., Lin, F., Xu, Y., Zhang, X., Li, Y., Wang, R., & Lai, L. (2007). Computation of octanol-water partition coefficients by guiding an additive model with knowledge. *Journal of Chemical Information and Modeling*, 47(6), 2140–2148. <https://doi.org/10.1021/ci700257y>
- Chien, E. Y. T., Liu, W., Zhao, Q., Katritch, V., Han, G. W., Hanson, M. A., Shi, L., Newman, A. H., Javitch, J. A., Cherezov, V., & Stevens, R. C. (2010). Structure of the human dopamine D3 receptor in complex with a D2/D3 selective antagonist. *Science (New York, N.Y.)*, 330(6007), 1091–1095. <https://doi.org/10.1126/science.1197410>
- Clark, D. E. (1999). Rapid calculation of polar molecular surface area and its application to the prediction of transport phenomena. 2. Prediction of blood-brain barrier penetration. *Journal of Pharmaceutical Sciences*, 88(8), 815–821. <https://doi.org/10.1021/jsp980402t>
- Clarke, Z. (2007). Emonapride. In S. J. Enna & D. B. Bylund (Eds.), *xPharm: The comprehensive pharmacology reference* (pp. 1–3). Elsevier. ISBN 9780080552323.
- Cobaugh, D. J., Erdman, A. R., Booze, L. L., Scharman, E. J., Christianson, G., Manoguerra, A. S., Caravati, E. M., Chyka, P. A., Woolf, A. D., Nelson, L. S., & Troutman, W. G. (2007). Atypical antipsychotic medication poisoning: An evidence-based consensus guideline for out-of-hospital management. *Clinical Toxicology (Philadelphia, PA)*, 45(8), 918–942. <https://doi.org/10.1080/15563650701665142>
- Cumming, J. G., Davis, A. M., Muresan, S., Haeberlein, M., & Chen, H. (2013). Chemical predictive modelling to improve compound quality. *Nature Reviews. Drug Discovery*, 12(12), 948–962. <https://doi.org/10.1038/nrd4128>
- Dallakyan, S., & Olson, A. J. (2015). Small-molecule library screening by docking with PyRx. *Methods in Molecular Biology (Clifton, N.J.)*, 1263, 243–250. https://doi.org/10.1007/978-1-4939-2269-7_19
- Dalpiaz, A., Gessi, S., Borea, P. A., & Gilli, G. (1995). Binding thermodynamics of serotonin to rat-brain 5-HT1A, 5HT2A and 5-HT3 receptors. *Life Sciences*, 57(12), PL141–146.
- de Bartolomeis, A., Barone, A., Begni, V., & Riva, M. A. (2022). Present and future antipsychotic drugs: A systematic review of the putative mechanisms of action for efficacy and a critical appraisal under a translational perspective. *Pharmacological Research*, 176, 106078. <https://doi.org/10.1016/J.PHRS.2022.106078>
- De las Cuevas, C., Sanz, E. J., Ruan, C. J., & de Leon, J. (2021). Clozapine-associated myocarditis in the World Health Organization's pharmacovigilance database: Focus on reports from various countries. *Revista de Psiquiatria y Salud Mental*, 15(4), 238–250. <https://doi.org/10.1016/j.rpsm.2021.07.004>
- De Leon, J. (2009). Pharmacogenomics: The promise of personalized medicine for CNS disorders. *Neuropsychopharmacology: Official Publication of the American College of Neuropsychopharmacology*, 34(1), 159–172. <https://doi.org/10.1038/npp.2008.147>
- Deng, C., & Dean, B. (2013). Mapping the pathophysiology of schizophrenia: Interactions between multiple cellular pathways. *Frontiers in Cellular Neuroscience*, 7, 238. <https://doi.org/10.3389/fncel.2013.00238>
- Durcan, M. J., Rigdon, G. C., Norman, M. H., & Morgan, P. F. (1995). Is clozapine selective for the dopamine D4 receptor? *Life Sciences*, 57(18), PL275–PL283. [https://doi.org/10.1016/0024-3205\(95\)02151-8](https://doi.org/10.1016/0024-3205(95)02151-8)
- Edwards, J. G., & Barnes, T. R. E. (1993). The side-effects of antipsychotic drugs. II. Effects on other physiological systems. *Antipsychotic drugs and their side-effects* (pp. 249–275). Academic Press.
- Edwards, S. J., & Smith, C. J. (2009). Tolerability of atypical antipsychotics in the treatment of adults with schizophrenia or bipolar disorder: A mixed treatment comparison of randomized controlled trials. *Clinical Therapeutics*, 31, 1345–1359. <https://doi.org/10.1016/j.clinthera.2009.07.004>
- Egan, W. J., Merz, K. M., & Baldwin, J. J. (2000). Prediction of drug absorption using multivariate statistics. *Journal of Medicinal Chemistry*, 43(21), 3867–3877. <https://doi.org/10.1021/jm000292e>
- Enoch, S. J., Ellison, C. M., Schultz, T. W., & Cronin, M. T. D. (2011). A review of the electrophilic reaction chemistry involved in covalent protein binding relevant to toxicity. *Critical Reviews in Toxicology*, 41(9), 783–802. <https://doi.org/10.3109/10408444.2011.598141>
- Ertl, P. (2021). Magic rings: Navigation in the ring chemical space guided by the bioactive rings. *Journal of Chemical Information and Modeling*, 62(9), 2164–2170. https://doi.org/10.1021/ACS.JCIM.1C00761/SUPPL_FILE/CI1C00761_SI_001.TXT
- Ertl, P., Rohde, B., & Selzer, P. (2000). Fast calculation of molecular polar surface area as a sum of fragment-based contributions and its application to the prediction of drug transport properties. *Journal of Medicinal Chemistry*, 43(20), 3714–3717. <https://doi.org/10.1021/jm000942e>
- Eugene, A. R., Eugene, B., Masiak, M., & Masiak, J. S. (2021). Head-to-head comparison of sedation and somnolence among 37 antipsychotics in schizophrenia, bipolar disorder, major depression, autism spectrum disorders, delirium, and repurposed in COVID-19, infectious diseases, and oncology from the FAERS, 2004–2020. *Frontiers in Pharmacology*, 12, 295. <https://doi.org/10.3389/fphar.2021.621691>
- Freedman, S. B., Patel, S., Marwood, R., Emms, F., Seabrook, G. R., Knowles, M. R., & McAllister, G. (1994). Expression and pharmacological characterization of the human D3 dopamine receptor. *The Journal of Pharmacology and Experimental Therapeutics*, 268(1), 417–426.
- Ganapathiraju, M. K., Thahir, M., Handen, A., Sarkar, S. N., Sweet, R. A., Nimgaonkar, V. L., Loscher, C. E., Bauer, E. M., & Chaparala, S. (2016). Schizophrenia interactome with 504 novel protein-protein interactions. *npj Schizophrenia*, 2, 1–10. <https://doi.org/10.1038/npjschz.2016.12>
- Gehlhaar, D. K., Verkhivker, G., Rejto, P. A., Fogel, D. B., Fogel, L. J., & Freer, S. T. (1995). Docking conformationally flexible small molecules into a protein binding site through evolutionary programming. In J. R. McDonnell, R. G. Reynolds, & D. B. Fogel (Eds.), *Evolutionary Programming IV: Proceedings of the Fourth Annual Conference on Evolutionary Programming* (pp. 615–627).
- Gleeson, M. P. (2008). Generation of a set of simple, interpretable ADMET rules of thumb. *Journal of Medicinal Chemistry*, 51(4), 817–834. <https://doi.org/10.1021/jm701122q>
- Haddad, C., Dib, J. E., Akl, N., Hallit, S., & Obeid, S. (2022). COVID-19 and psychosis, depression, obsession and quality of life in Lebanese patients with schizophrenia: Any changes after 5 months of quarantine? *BMC Psychology*, 10, 1–10. <https://doi.org/10.1186/s40359-022-00750-7>
- Hall, H., Köhler, C., & Gawell, L. (1985). Some in vitro receptor binding properties of [3H]etoclopride, a novel substituted benzamide, selective for dopamine-D2 receptors in the rat brain. *European Journal of Pharmacology*, 111(2), 191–199. [https://doi.org/10.1016/0014-2999\(85\)90756-3](https://doi.org/10.1016/0014-2999(85)90756-3)
- Hall, H., Sällemark, M., & Jerning, E. (1986). Effects of remoxipride and some related new substituted salicylamides on rat brain receptors. *Acta Pharmacologica et Toxicologica*, 58(1), 61–70. <https://doi.org/10.1111/j.1600-0773.1986.tb00071.x>
- Hanley, J. A., & McNeil, B. J. (1982). The meaning and use of the area under a receiver operating characteristic (ROC) curve. *Radiology*, 143(1), 29–36. <https://doi.org/10.1148/radiology.143.1.7063747>
- Harding, S. D., Armstrong, J. F., Faccenda, E., Southan, C., Alexander, S. P. H., Davenport, A. P., Pawson, A. J., Spedding, M., & Davies, J. A., NC-IUPHAR. (2022). The IUPHAR/BPS guide to PHARMACOLOGY in 2022: Curating pharmacology for COVID-19, malaria and antibacterials. *Nucleic Acids Research*, 50(D1), D1282–D1294. <https://doi.org/10.1093/nar/gkab1010>
- Harel, S., & Radinsky, K. (2018). Prototype-based compound discovery using deep generative models. *Molecular Pharmaceutics*, 15(10), 4406–4416. <https://doi.org/10.1021/acs.molpharmaceut.8b00474>
- Harris, A. (2020). A brief guide to medications for psychosis. *A clinical introduction to psychosis* (pp. 537–560). Elsevier. ISBN 9780128150122.
- Heron, P., Spanakis, P., Crostrand, S., Johnston, G., Newbronner, E., Wadman, R., Walker, L., Gilbody, S., & Peckham, E. (2022). Loneliness among people with severe mental illness during the COVID-19

- pandemic: Results from a linked UK population cohort study. *PLoS One*, 17(1), e0262363. <https://doi.org/10.1371/journal.pone.0262363>
- Horvath, D., Lisurek, M., Rupp, B., Kühne, R., Specker, E., von Kries, J., Rognan, D., Andersson, C. D., Almqvist, F., Elofsson, M., Enqvist, P.-A., Gustavsson, A.-L., Remez, N., Mestres, J., Marcou, G., Varnek, A., Hibert, M., Quintana, J., & Frank, R. (2014). Design of a general-purpose European compound screening library for EU-OPENSCREEN. *ChemMedChem*, 9(10), 2309–2326. <https://doi.org/10.1002/cmdc.201402126>
- Hu, Y., Zhang, H., Wang, H., Wang, C., Kung, S., & Li, C. (2022). Adjunctive antidepressants for the acute treatment of bipolar depression: A systematic review and meta-analysis. *Psychiatry Research*, 311, 114468. <https://doi.org/10.1016/j.psychres.2022.114468>
- Hughes, J. D., Blagg, J., Price, D. A., Bailey, S., Decrescenzo, G. A., Devraj, R. V., Ellsworth, E., Fobian, Y. M., Gibbs, M. E., Gilles, R. W., Greene, N., Huang, E., Krieger-Burke, T., Loesel, J., Wager, T., Whiteley, L., & Zhang, Y. (2008). Physicochemical drug properties associated with in vivo toxicological outcomes. *Bioorganic & Medicinal Chemistry Letters*, 18(17), 4872–4875. <https://doi.org/10.1016/j.bmcl.2008.07.071>
- Irwin, J. J., & Shoichet, B. K. (2005). ZINC – A free database of commercially available compounds for virtual screening. *Journal of Chemical Information and Modeling*, 45(1), 177–182. <https://doi.org/10.1021/ci049714+>
- Jayaraj, J. M., Jothimani, M., Palanisamy, C. P., Pentikäinen, O. T., Pannipara, M., Al-Sehemi, A. G., Muthusamy, K., & Gopinath, K. (2022). Computational study on the inhibitory effect of natural compounds against the SARS-CoV-2 proteins. *Bioinorganic Chemistry and Applications*, 2022, 1–19. <https://doi.org/10.1155/2022/8635054>
- Jeffrey, P., & Summerfield, S. (2010). Assessment of the blood-brain barrier in CNS drug discovery. *Neurobiology of Disease*, 37(1), 33–37. <https://doi.org/10.1016/j.nbd.2009.07.033>
- Jo, S., Kim, T., Iyer, V. G., & Im, W. (2008). CHARMM-GUI: A web-based graphical user interface for CHARMM. *Journal of Computational Chemistry*, 29(11), 1859–1865. <https://doi.org/10.1002/jcc.20945>
- Jongsma, H. E., Turner, C., Kirkbride, J. B., & Jones, P. B. (2019). International incidence of psychotic disorders, 2002–17: A systematic review and meta-analysis. *The Lancet. Public Health*, 4(5), e229–e244. [https://doi.org/10.1016/S2468-2667\(19\)30056-8](https://doi.org/10.1016/S2468-2667(19)30056-8)
- Kim, D. H., & Stahl, S. M. (2010). Antipsychotic drug development. *Current topics in behavioral neurosciences* (Vol. 4, pp. 124–139). Springer. ISBN 9783642137167.
- Kimura, K. T., Asada, H., Inoue, A., Kadji, F. M. N., Im, D., Mori, C., Arakawa, T., Hirata, K., Nomura, Y., Nomura, N., Aoki, J., Iwata, S., & Shimamura, T. (2019). Structures of the 5-HT_{2A} receptor in complex with the antipsychotics risperidone and zotepine. *Nature Structural & Molecular Biology*, 26(2), 121–128. <https://doi.org/10.1038/s41594-018-0180-z>
- Kondej, M., Stepnicki, P., & Kaczor, A. A. (2018). Multi-target approach for drug discovery against schizophrenia. *International Journal of Molecular Sciences*, 19, 3105. <https://doi.org/10.3390/ijms19103105>
- Kongsamut, S., Kang, J., Chen, X. L., Roehr, J., & Rampe, D. (2002). A comparison of the receptor binding and HERG channel affinities for a series of antipsychotic drugs. *European Journal of Pharmacology*, 450(1), 37–41. [https://doi.org/10.1016/S0014-2999\(02\)02074-5](https://doi.org/10.1016/S0014-2999(02)02074-5)
- Kroese, W. K., Hufiesen, S. J., Popadak, B. A., Renock, S. M., Steinberg, S., Ernsberger, P., Jayathilake, K., Meltzer, H. Y., & Roth, B. L. (2003). HL-Histamine receptor affinity predicts short-term weight gain for typical and atypical antipsychotic drugs. *Neuropsychopharmacology: Official Publication of the American College of Neuropsychopharmacology*, 28(3), 519–526. <https://doi.org/10.1038/sj.npp.1300027>
- Kučerka, N., Tristram-Nagle, S., & Nagle, J. F. (2005). Structure of fully hydrated fluid phase lipid bilayers with monounsaturated chains. *The Journal of Membrane Biology*, 208(3), 193–202. <https://doi.org/10.1007/s00232-005-7006-8>
- Kunwittaya, S., Nantasenamat, C., Treeratanapiboon, L., Srisarin, A., Isarankura-Na-Ayudhya, C., & Prachayasittikul, V. (2013). Influence of logBB cut-off on the prediction of blood-brain barrier permeability. *Biomedical and Applied Technology Journal*, 1, 16–34.
- Lagorce, D., Bouslama, L., Becot, J., Miteva, M. A., & Villoutreix, B. O. (2017). FAF-Drugs4: Free ADME-tox filtering computations for chemical biology and early stages drug discovery. *Bioinformatics (Oxford, England)*, 33(22), 3658–3660. <https://doi.org/10.1093/bioinformatics/btx491>
- Lagorce, D., Douguet, D., Miteva, M. A., & Villoutreix, B. O. (2017). Computational analysis of calculated physicochemical and ADMET properties of protein-protein interaction inhibitors. *Scientific Reports*, 7, 46277. <https://doi.org/10.1038/srep46277>
- Lagorce, D., Sperario, O., Baell, J. B., Miteva, M. A., & Villoutreix, B. O. (2015). FAF-Drugs3: A web server for compound property calculation and chemical library design. *Nucleic Acids Research*, 43(W1), W200–W207. <https://doi.org/10.1093/nar/gkv353>
- Lahti, R. A., Evans, D. L., Stratman, N. C., & Figur, L. M. (1993). Dopamine D4 versus D2 receptor selectivity of dopamine receptor antagonists: Possible therapeutic implications. *European Journal of Pharmacology*, 236(3), 483–486. [https://doi.org/10.1016/0014-2999\(93\)90488-4](https://doi.org/10.1016/0014-2999(93)90488-4)
- Leo, A. J. (1993). Calculating log P_{oct} from structures. *Chemical Reviews*, 93(4), 1281–1306. <https://doi.org/10.1021/cr00020a001>
- Lesage, A. S., Wouters, R., Van Gompel, P., Heylen, L., Vanhoenacker, P., Haegeman, G., Luyten, W., & Lesen, J. E. (1998). Agonistic properties of alniditan, sumatriptan and dihydroergotamine on human 5-HT(1B) and 5-HT(1D) receptors expressed in various mammalian cell lines. *British Journal of Pharmacology*, 123(8), 1655–1665. <https://doi.org/10.1038/sj.bjp.0701766>
- Leysen, J. E., Gommeren, W., Heylen, L., Luyten, W. H., Van de Weyer, I., Vanhoenacker, P., Haegeman, G., Schotte, A., Van Gompel, P., Wouters, R., & Lesage, A. S. (1996). Alniditan, a new 5-Hydroxytryptamine1D agonist and migraine-abortive agent: Ligand-binding properties of human 5-hydroxytryptamine1D α , human 5-Hydroxytryptamine1D β , and calf 5-hydroxytryptamine1D receptors investigated with [³H]5-hydroxytryptamine and [³H]. *Molecular Pharmacology*, 50(6), 1567–1580.
- Lipinski, C. A. (2005). Chapter 11 filtering in drug discovery. *Annual reports in computational chemistry* (Vol. 1, pp. 155–168). Elsevier.
- Lipinski, C. A. (2016). Rule of five in 2015 and beyond: Target and ligand structural limitations, ligand chemistry structure and drug discovery project decisions. *Advanced Drug Delivery Reviews*, 101, 34–41. <https://doi.org/10.1016/j.addr.2016.04.029>
- Lipinski, C. A., Lombardo, F., Dominy, B. W., & Feeney, P. J. (2001). Experimental and computational approaches to estimate solubility and permeability in drug discovery and development settings. 1P11 of original article: S0169-409X(96)00423-1. The article was originally published in Advanced Drug Delivery Reviews 23 (1997). *Advanced Drug Delivery Reviews*, 46(1–3), 3–26. [https://doi.org/10.1016/S0169-409X\(00\)00129-0](https://doi.org/10.1016/S0169-409X(00)00129-0)
- Lipinski, C. A., Lombardo, F., Dominy, B. W., & Feeney, P. J. (2012). Experimental and computational approaches to estimate solubility and permeability in drug discovery and development settings. *Advanced Drug Delivery Reviews*, 64, 4–17. <https://doi.org/10.1016/j.addr.2012.09.019>
- Liu, R., Li, X., & Lam, K. S. (2017). Combinatorial chemistry in drug discovery. *Current Opinion in Chemical Biology*, 38, 117–126. <https://doi.org/10.1016/j.cbpa.2017.03.017>
- Lovering, F., Bikker, J., & Humbert, C. (2009). Escape from flatland: Increasing saturation as an approach to improving clinical success. *Journal of Medicinal Chemistry*, 52(21), 6752–6756. <https://doi.org/10.1021/jm901241e>
- MacKenzie, R. G., VanLeeuwen, D., Pugsley, T. A., Shih, Y. H., Demattos, S., Tang, L., Todd, R. D., & O’Malley, K. L. (1994). Characterization of the human dopamine D3 receptor expressed in transfected cell lines. *European Journal of Pharmacology*, 266(1), 79–85. [https://doi.org/10.1016/0922-4106\(94\)90212-7](https://doi.org/10.1016/0922-4106(94)90212-7)
- McCutcheon, R. A., Reis Marques, T., & Howes, O. D. (2020). Schizophrenia—An overview. *JAMA Psychiatry*, 77(2), 201–210. <https://doi.org/10.1001/jamapsychiatry.2019.3360>
- McGowan, O. O., & Reynolds, G. P. (2020). Functional pharmacogenetics of serotonin receptors in psychiatric drug action. *Handbook of behavioral neuroscience* (Vol. 31, pp. 941–957). Elsevier.
- Mierau, J., Schneider, F. J., Ensinger, H. A., Chio, C. L., Lajiness, M. E., & Huff, R. M. (1995). Pramipexole binding and activation of cloned and expressed dopamine D₂, D₃ and D₄ receptors. *European Journal of*

- Pharmacology*, 290(1), 29–36. [https://doi.org/10.1016/0922-4106\(95\)90013-6](https://doi.org/10.1016/0922-4106(95)90013-6)
- Millan, M. J., Brocco, M., Gobert, A., Schreiber, R., & Dekeyne, A. (1999). S-16924 [(R)-2-{1-[2-(2,3-dihydro-benzo[1,4]dioxin-5-yloxy)ethyl]- pyrrolidin-3-yl}-1-(4-fluorophenyl)-ethanone], a novel, potential antipsychotic with marked serotonin(1A) agonist properties: III. Anxiolytic actions in comparison with clozapine and haloperidol. *Journal of Pharmacology and Experimental Therapeutics*, 288, 1002–1014.
- Millan, M. J., Peglion, J. L., Vian, J., Rivet, J. M., Brocco, M., Gobert, A., Newman-Tancredi, A., Dacquet, C., Bervoets, K., & Girardon, S. (1995). Functional correlates of dopamine D3 receptor activation in the rat *in vivo* and their modulation by the selective antagonist, (+)-S 14297: I. Activation of postsynaptic D3 receptors mediates hypothermia, whereas blockade of D2 receptors elicits prolactin. *Journal of Pharmacology and Experimental Therapeutics*, 275, 885–898.
- Mok, N. Y., Maxe, S., & Brenk, R. (2013). Locating sweet spots for screening hits and evaluating pan-assay interference filters from the performance analysis of two lead-like libraries. *Journal of Chemical Information and Modeling*, 53(3), 534–544. <https://doi.org/10.1021/ci300382f>
- Moons, T., De Roo, M., Claes, S., & Dom, G. (2011). Relationship between P-glycoprotein and second-generation antipsychotics. *Pharmacogenomics*, 12(8), 1193–1211. <https://doi.org/10.2217/pgs.11.55>
- Moreno-Küstner, B., Martín, C., & Pastor, L. (2018). Prevalence of psychotic disorders and its association with methodological issues. A systematic review and meta-analyses. *PLoS One*, 13(4), e0195687. <https://doi.org/10.1371/journal.pone.0195687>
- Morris, G. M., Goodsell, D. S., Halliday, R. S., Huey, R., Hart, W. E., Belew, R. K., & Olson, A. J. (1998). Automated docking using a Lamarckian genetic algorithm and an empirical binding free energy function. *Journal of Computational Chemistry*, 19(14), 1639–1662. [https://doi.org/10.1002/\(SICI\)1096-987X\(19981115\)19:14<1639::AID-JCC10>3.0.CO;2-B](https://doi.org/10.1002/(SICI)1096-987X(19981115)19:14<1639::AID-JCC10>3.0.CO;2-B)
- Muehlbacher, M., Spitzer, G. M., Liedl, K. R., & Kornhuber, J. (2011). Qualitative prediction of blood-brain barrier permeability on a large and refined dataset. *Journal of Computer-Aided Molecular Design*, 25(12), 1095–1106. <https://doi.org/10.1007/s10822-011-9478-1>
- Mwesiga, E. K., Nakasujja, N., Muhwezi, W. W., & Musisi, S. (2021). The COVID-19 pandemic has reinforced the need for community mental health-care models in Uganda. *The Lancet. Psychiatry*, 8(5), 362. [https://doi.org/10.1016/S2215-0366\(21\)00070-5](https://doi.org/10.1016/S2215-0366(21)00070-5)
- Mwesiga, E. K., Nakasujja, N., Nakku, J., Nanyonga, A., Gumikiriza, J. L., Bangirana, P., Akena, D., & Musisi, S. (2020). One year prevalence of psychotic disorders among first treatment contact patients at the National Psychiatric Referral and Teaching Hospital in Uganda. *Plos One*, 15(1), e0218843. <https://doi.org/10.1371/journal.pone.0218843>
- Oka, T., Kubo, T., Kobayashi, N., Nakai, F., Miyake, Y., Hamamura, T., Honjo, M., Toda, H., Boku, S., Kanazawa, T., et al. (2021). Multiple time measurements of multidimensional psychiatric states from immediately before the COVID-19 pandemic to one year later: A longitudinal online survey of the Japanese population. *Translational Psychiatry*, 11, 1–8. <https://doi.org/10.1038/s41398-021-01696-x>
- Oprea, T. I. (2000). Property distribution of drug-related chemical databases. *Journal of Computer-Aided Molecular Design*, 14(3), 251–264. <https://doi.org/10.1023/A:1008130001697>
- Oprea, T. I., Davis, A. M., Teague, S. J., & Leeson, P. D. (2001). Is there a difference between leads and drugs? A historical perspective. *Journal of Chemical Information and Computer Sciences*, 41(5), 1308–1315. <https://doi.org/10.1021/ci010366a>
- Pence, A. Y., Pries, L.-K., Ferrara, M., Rutten, B. P. F., van Os, J., & Guloksuz, S. (2022). Gender differences in the association between environment and psychosis. *Schizophrenia Research*, 243, 120–137. <https://doi.org/10.1016/j.schres.2022.02.039>
- Pihan, E., Colliandre, L., Guichou, J.-F., & Douguet, D. (2012). e-Drug3D: 3D structure collections dedicated to drug repurposing and fragment-based drug design. *Bioinformatics (Oxford, England)*, 28(11), 1540–1541. <https://doi.org/10.1093/bioinformatics/bts186>
- Pires, D. E. V., Blundell, T. L., & Ascher, D. B. (2015). pkCSM: Predicting small-molecule pharmacokinetic and toxicity properties using graph-based signatures. *Journal of Medicinal Chemistry*, 58(9), 4066–4072. <https://doi.org/10.1021/acs.jmedchem.5b00104>
- Platts, J. A., Abraham, M. H., Zhao, Y. H., Hersey, A., Ijaz, L., & Butina, D. (2001). Correlation and prediction of a large blood-brain distribution data set—An LFER study. *European Journal of Medicinal Chemistry*, 36(9), 719–730. [https://doi.org/10.1016/s0223-5234\(01\)01269-7](https://doi.org/10.1016/s0223-5234(01)01269-7)
- Polito, N. B., & Fellows, S. E. (2017). Pharmacologic interventions for intractable and persistent hiccups: A systematic review. *The Journal of Emergency Medicine*, 53(4), 540–549. <https://doi.org/10.1016/j.jemermed.2017.05.033>
- Potashman, M. H., & Duggan, M. E. (2009). Covalent modifiers: An orthogonal approach to drug design. *Journal of Medicinal Chemistry*, 52(5), 1231–1246. <https://doi.org/10.1021/jm8008597>
- Przybylak, K. R., Alzahrani, A. R., & Cronin, M. T. D. (2014). How does the quality of phospholipidosis data influence the predictivity of structural alerts? *Journal of Chemical Information and Modeling*, 54(8), 2224–2232. <https://doi.org/10.1021/ci500233k>
- Reynès, C., Host, H., Camproux, A.-C., Laconde, G., Leroux, F., Mazars, A., Deprez, B., Fahraeus, R., Villoutreix, B. O., & Sperandio, O. (2010). Designing focused chemical libraries enriched in protein-protein interaction inhibitors using machine-learning methods. *PLoS Computational Biology*, 6(3), e1000695. <https://doi.org/10.1371/journal.pcbi.1000695>
- Rishton, G. M. (2003). Nonleadlikeness and leadlikeness in biochemical screening. *Drug Discovery Today*, 8(2), 86–96. <https://doi.org/10.1016/S1359-644602025722>
- Rishton, G. M., LaBonte, K., Williams, A. J., Kassam, K., & Kolovanov, E. (2006). Computational approaches to the prediction of blood-brain barrier permeability: A comparative analysis of central nervous system drugs versus secretase inhibitors for Alzheimer's disease. *Current Opinion in Drug Discovery & Development*, 9, 303–313.
- Roberts, D. W., & Natsch, A. (2009). High throughput kinetic profiling approach for covalent binding to peptides: Application to skin sensitization potency of Michaelis acceptor electrophiles. *Chemical Research in Toxicology*, 22(3), 592–603. <https://doi.org/10.1021/tx800431x>
- Roffman, J. L., & Pirl, W. F. (2003). Use of antipsychotic medication in chemotherapy-induced nausea and vomiting. *Expert Review of Neurotherapeutics*, 3(1), 77–84. <https://doi.org/10.1586/14737175.3.1.77>
- Roper, C., & Tanguay, R. L. (2020). Tox21 and adverse outcome pathways. *An introduction to interdisciplinary toxicology* (pp. 559–568). Academic Press.
- Roth, B. L., Sheffler, D. J., & Kroeze, W. K. (2004). Magic shotguns versus magic bullets: Selectively non-selective drugs for mood disorders and schizophrenia. *Nature Reviews. Drug Discovery*, 3(4), 353–359. <https://doi.org/10.1038/nrd1346>
- Ryckaert, J. P., Cicotti, G., & Berendsen, H. J. C. (1977). Numerical integration of the cartesian equations of motion of a system with constraints: Molecular dynamics of n-alkanes. *Journal of Computational Physics*, 23(3), 327–341. [https://doi.org/10.1016/0021-9991\(77\)90098-5](https://doi.org/10.1016/0021-9991(77)90098-5)
- Salomon-Ferrer, R., Case, D. A., & Walker, R. C. (2013). An overview of the Amber biomolecular simulation package. *Wiley Interdisciplinary Reviews: Computational Molecular Science*, 3(2), 198–210. <https://doi.org/10.1002/wcms.1121>
- Saudemont, G., Prod'Homme, C., Da Silva, A., Villet, S., Reich, M., Penel, N., & Gamblin, V. (2020). The use of olanzapine as an antiemetic in palliative medicine: A systematic review of the literature. *BMC Palliative Care*, 19, 1–11. <https://doi.org/10.1186/S12904-020-00559-4/TABLES/2>
- Schotte, A., Janssen, P. F. M., Gommeren, W., Luyten, W., Van Gompel, P., Lesage, A. S., De Loore, K., & Leysen, J. E. (1996). Risperidone compared with new and reference antipsychotic drugs: In vitro and in vivo receptor binding. *Psychopharmacology*, 124(1-2), 57–73. <https://doi.org/10.1007/BF02245606>
- Schüller, A., Schneider, G., & Byvatov, E. (2003). SMILIB: Rapid assembly of combinatorial libraries in SMILES notation. *QSAR & Combinatorial Science*, 22, 719–721. <https://doi.org/10.1002/qsar.200310008>
- Seale, C., Chaplin, R., Lelliott, P., & Quirk, A. (2007). Antipsychotic medication, sedation and mental clouding: An observational study of psychiatric consultations. *Social Science & Medicine* (1982), 65(4), 698–711. <https://doi.org/10.1016/j.soscimed.2007.03.047>

- Seeman, P., Guan, H. -C., Van Tol, H. H. M., & Niznik, H. B. (1993). Low density of dopamine D4 receptors in Parkinson's, schizophrenia, and control brain striata. *Synapse (New York, N.Y.)*, 14(4), 247–253. <https://doi.org/10.1002/syn.890140402>
- Sekhar, G. N., Fleckney, A. L., Boyanova, S. T., Rupawala, H., Lo, R., Wang, H., Farag, D. B., Rahman, K. M., Broadstock, M., Reeves, S., & Thomas, S. A. (2019). Region-specific blood-brain barrier transporter changes leads to increased sensitivity to amisulpride in Alzheimer's disease. *Fluids and Barriers of the CNS*, 16(1), 38. <https://doi.org/10.1186/s12987-019-0158-1>
- Shahid, M., Walker, G. B., Zorn, S. H., & Wong, E. H. F. (2009). Asenapine: A novel psychopharmacologic agent with a unique human receptor signature. *Journal of Psychopharmacology (Oxford, England)*, 23(1), 65–73. <https://doi.org/10.1177/0269881107082944>
- Shen, J., Cheng, F., Xu, Y., Li, W., & Tang, Y. (2010). Estimation of ADME properties with substructure pattern recognition. *Journal of Chemical Information and Modeling*, 50(6), 1034–1041. <https://doi.org/10.1021/ci100104j>
- Shityakov, S., & Förster, C. (2014). In silico predictive model to determine vector-mediated transport properties for the blood-brain barrier choline transporter. *Advances and Applications in Bioinformatics and Chemistry : AACB*, 7, 23–36. <https://doi.org/10.2147/AACB.S63749>
- Shityakov, S., Salvador, E., Pastorin, G., & Förster, C. (2015). Blood-brain barrier transport studies, aggregation, and molecular dynamics simulation of multiwalled carbon nanotube functionalized with fluorescein isothiocyanate. *International Journal of Nanomedicine*, 10, 1703–1713. <https://doi.org/10.2147/IJN.S68429>
- Simons, P., Cosgrove, L., Shaughnessy, A. F., & Bursztajn, H. (2017). Antipsychotic augmentation for major depressive disorder: A review of clinical practice guidelines. *International Journal of Law and Psychiatry*, 55, 64–71. <https://doi.org/10.1016/j.ijlp.2017.10.003>
- Singh, N., Guha, R., Giulianotti, M. A., Pinilla, C., Houghten, R. A., & Medina-Franco, J. L. (2009). Chemoinformatic analysis of combinatorial libraries, drugs, natural products, and molecular libraries small molecule repository. *Journal of Chemical Information and Modeling*, 49(4), 1010–1024. <https://doi.org/10.1021/ci800426u>
- Sivakumar, K. C., Haixiao, J., Naman, C. B., & Sajeevan, T. P. (2020). Prospects of multitarget drug designing strategies by linking molecular docking and molecular dynamics to explore the protein-ligand recognition process. *Drug Development Research*, 81(6), 685–699. <https://doi.org/10.1002/ddr.21673>
- Smith, G. F. (2011). Designing drugs to avoid toxicity. *Progress in Medicinal Chemistry*, 50, 1–47. <https://doi.org/10.1016/B978-0-12-381290-2.00001-X>
- Sokoloff, P., Andrieux, M., Besançon, R., Pilon, C., Martres, M. P., Giros, B., & Schwartz, J. C. (1992). Pharmacology of human dopamine D3 receptor expressed in a mammalian cell line: Comparison with D2 receptor. *European Journal of Pharmacology*, 225(4), 331–337. [https://doi.org/10.1016/0922-4106\(92\)90107-7](https://doi.org/10.1016/0922-4106(92)90107-7)
- Sperandio, O., Reynès, C. H., Camproux, A.-C., & Villoutreix, B. O. (2010). Rationalizing the chemical space of protein-protein interaction inhibitors. *Drug Discovery Today*, 15(5–6), 220–229. <https://doi.org/10.1016/j.drudis.2009.11.007>
- Stepan, A. F., Walker, D. P., Bauman, J., Price, D. A., Baillie, T. A., Kalgutkar, A. S., & Aleo, M. D. (2011). Structural alert/reactive metabolite concept as applied in medicinal chemistry to mitigate the risk of idiosyncratic drug toxicity: A perspective based on the critical examination of trends in the top 200 drugs marketed in the United States. *Chemical Research in Toxicology*, 24(9), 1345–1410. <https://doi.org/10.1021/tx200168d>
- Stroup, T. S., & Gray, N. (2018). Management of common adverse effects of antipsychotic medications. *World Psychiatry: Official Journal of the World Psychiatric Association (WPA)*, 17(3), 341–356. <https://doi.org/10.1002/wps.20567>
- Subramaniam, M., Abdin, E., Vaingankar, J. A., Sambasivam, R., Zhang, Y. J., Shafie, S., Basu, S., Chan, C. T., Tan, C. S., Verma, S. K., et al. (2021). Lifetime prevalence and correlates of schizophrenia and other psychotic disorders in Singapore. *Frontiers in Psychiatry*, 12, 249. <https://doi.org/10.3389/fpsyg.2021.650674>
- Suenderhauf, C., Hammann, F., & Huwyler, J. (2012). Computational prediction of blood-brain barrier permeability using decision tree induction. *Molecules*, 17(9), 10429–10445. <https://doi.org/10.3390/molecules170910429>
- Tamaian, R., Niculescu, V. C., & Anghel, M. (2010). In silico predictions for improving permeability properties of principal anticancer anthracyclines through structural modification. *Bulletin of University of Agricultural Sciences and Veterinary Medicine*, 67, 329–336.
- Tang, L., Todd, R. D., Heller, A., & O'Malley, K. L. (1994). Pharmacological and functional characterization of D2, D3 and D4 dopamine receptors in fibroblast and dopaminergic cell lines. *Journal of Pharmacology and Experimental Therapeutics*, 268, 495–502.
- Taquet, M., Luciano, S., Geddes, J. R., & Harrison, P. J. (2021). Bidirectional associations between COVID-19 and psychiatric disorder: Retrospective cohort studies of 62354 COVID-19 cases in the USA. *The Lancet. Psychiatry*, 8(2), 130–140. [https://doi.org/10.1016/S2215-0366\(20\)30462-4](https://doi.org/10.1016/S2215-0366(20)30462-4)
- Taylor, R. D., MacCoss, M., & Lawson, A. D. G. (2017). Combining molecular scaffolds from FDA approved drugs: Application to drug discovery. *Journal of Medicinal Chemistry*, 60(5), 1638–1647. <https://doi.org/10.1021/acs.jmedchem.6b01367>
- Thanontip, K., Chetsawang, B., & Chumchua, V. (2019). Novel protein-protein interaction network of antipsychotic drugs and cognitive function. Proceedings of the BMEiCON 2019 - 12th Biomedical Engineering International Conference; Institute of Electrical and Electronics Engineers Inc.
- Thomsen, R., & Christensen, M. H. (2006). MolDock: A new technique for high-accuracy molecular docking. *Journal of Medicinal Chemistry*, 49(11), 3315–3321. <https://doi.org/10.1021/jm051197e>
- Tice, M. A. B., Hashemi, T., Taylor, L. A., Duffy, R. A., & McQuade, R. D. (1994). Characterization of the binding of SCH 39166 to the five cloned dopamine receptor subtypes. *Pharmacology, Biochemistry, and Behavior*, 49(3), 567–571. [https://doi.org/10.1016/0091-3057\(94\)90070-1](https://doi.org/10.1016/0091-3057(94)90070-1)
- Todeschini, R., & Consonni, V. (2008). In R. Mannhold, H. Kubinyi, H. Timmerman (Eds.), *Handbook of Molecular Descriptors*. WILEY-VCH Verlag GmbH. ISBN 9783527613106.
- Trott, O., & Olson, A. J. (2010). AutoDock Vina: Improving the speed and accuracy of docking with a new scoring function, efficient optimization, and multithreading. *Journal of Computational Chemistry*, 31(2), 455–461. <https://doi.org/10.1002/jcc.21334>
- Vanover, K. E., Harvey, S. C., Son, T., Bradley, S. R., Kold, H., Makhay, M., Veinbergs, I., Spalding, T. A., Weiner, D. M., Andersson, C. M., Tolf, B.-R., Brann, M. R., Hacksell, U., & Davis, R. E. (2004). Pharmacological characterization of AC-90179 [2-(4-methoxy-phenyl)-N-(4-methyl-benzyl)-N-(1-methyl-piperidin-4-yl)-acetamide hydrochloride]: A selective serotonin 2A receptor inverse agonist. *The Journal of Pharmacology and Experimental Therapeutics*, 310(3), 943–951. <https://doi.org/10.1124/jpet.104.066688>
- Veber, D. F., Johnson, S. R., Cheng, H.-Y., Smith, B. R., Ward, K. W., & Kopple, K. D. (2002). Molecular properties that influence the oral bioavailability of drug candidates. *Journal of Medicinal Chemistry*, 45(12), 2615–2623. <https://doi.org/10.1021/jm020017n>
- Wacker, D., Wang, S., McCorry, J. D., Betz, R. M., Venkatakrishnan, A. J., Levit, A., Lansu, K., Schools, Z. L., Che, T., Nichols, D. E., Shoichet, B. K., Dror, R. O., & Roth, B. L. (2017). Crystal structure of an LSD-bound human serotonin receptor. *Cell*, 168(3), 377–389.e12. <https://doi.org/10.1016/j.cell.2016.12.033>
- Wang, S., Che, T., Levit, A., Shoichet, B. K., Wacker, D., & Roth, B. L. (2018). Structure of the D2 dopamine receptor bound to the atypical antipsychotic drug risperidone. *Nature*, 555(7695), 269–273. <https://doi.org/10.1038/nature25758>
- Wang, Z., Chen, Y., Liang, H., Bender, A., Glen, R. C., & Yan, A. (2011). P-glycoprotein substrate models using support vector machines based on a comprehensive data set. *Journal of Chemical Information and Modeling*, 51(6), 1447–1456. <https://doi.org/10.1021/ci2001583>
- Wang, S.-M., Han, C., Lee, S.-J., Jun, T.-Y., Patkar, A. A., Masand, P. S., & Pae, C.-U. (2016). Second generation antipsychotics in the treatment of major depressive disorder: An update. *Chonnam Medical Journal*, 52(3), 159–172. <https://doi.org/10.4068/CMJ.2016.52.3.159>

- Wang, C., Jiang, Y., Ma, J., Wu, H., Wacker, D., Katritch, V., Han, G. W., Liu, W., Huang, X.-P., Vardy, E., McCory, J. D., Gao, X., Zhou, X. E., Melcher, K., Zhang, C., Bai, F., Yang, H., Yang, L., Jiang, H., ... Xu, H. E. (2013). Structural basis for molecular recognition at serotonin receptors. *Science (New York, N.Y.)*, 340(6132), 610–614. <https://doi.org/10.1126/science.1232807>
- Wang, P., & Si, T. (2013). Use of antipsychotics in the treatment of depressive disorders. *Shanghai Archives of Psychiatry*, 25(3), 134–140. <https://doi.org/10.3969/j.issn.1002-0829.2013.03.002>
- Wang, S., Wacker, D., Levit, A., Che, T., Betz, R. M., McCory, J. D., Venkatakrishnan, A. J., Huang, X.-P., Dror, R. O., Shoichet, B. K., & Roth, B. L. (2017). D4 dopamine receptor high-resolution structures enable the discovery of selective agonists. *Science (New York, N.Y.)*, 358(6361), 381–386. <https://doi.org/10.1126/science.aan5468>
- Wang, B., Zartaloudi, E., Linden, J. F., & Bramon, E. (2022). Neurophysiology in psychosis: The quest for disease biomarkers. *Translational Psychiatry*, 12(1), 10. <https://doi.org/10.1038/s41398-022-01860-x>
- Weininger, D. (1988). SMILES, a chemical language and information system: 1: Introduction to methodology and encoding rules. *Journal of Chemical Information and Computer Science*, 28, 31–36. <https://doi.org/10.1021/ci00057a005>
- Xu, P., Huang, S., Zhang, H., Mao, C., Zhou, X. E., Cheng, X., Simon, I. A., Shen, D.-D., Yen, H.-Y., Robinson, C. V., Harpsøe, K., Svensson, B., Guo, J., Jiang, H., Gloriam, D. E., Melcher, K., Jiang, Y., Zhang, Y., & Xu, H. E. (2021). Structural insights into the lipid and ligand regulation of serotonin receptors. *Nature*, 592(7854), 469–473. <https://doi.org/10.1038/s41586-021-03376-8>
- Yan, A., Liang, H., Chong, Y., Nie, X., & Yu, C. (2013). In-silico prediction of blood-brain barrier permeability. *SAR and QSAR in Environmental Research*, 24(1), 61–74. <https://doi.org/10.1080/1062936X.2012.729224>
- Yang, F., Ma, Q., Ma, B., Jing, W., Liu, J., Guo, M., Li, J., Wang, Z., & Liu, M. (2021). Dyslipidemia prevalence and trends among adult mental disorder inpatients in Beijing, 2005–2018: A longitudinal observational study. *Asian Journal of Psychiatry*, 57, 102583. <https://doi.org/10.1016/j.ajp.2021.102583>
- Zhang, W., Pei, J., & Lai, L. (2017). Computational multitarget drug design. *Journal of Chemical Information and Modeling*, 57(3), 403–412. <https://doi.org/10.1021/acs.jcim.6b00491>